LA-UR-04-4778

E.L.Vold

Compressible aspects in simulations of multi-mode Rayleigh-Taylor mixing

Erik L. Vold
w/ A.J. Scannapieco, T.T. Clark, C.W. Cranfill

Presentation to the IWPCTM9
Cambridge, UK, July 19-23, 2004

compressible multifluid computations | incompressible computations

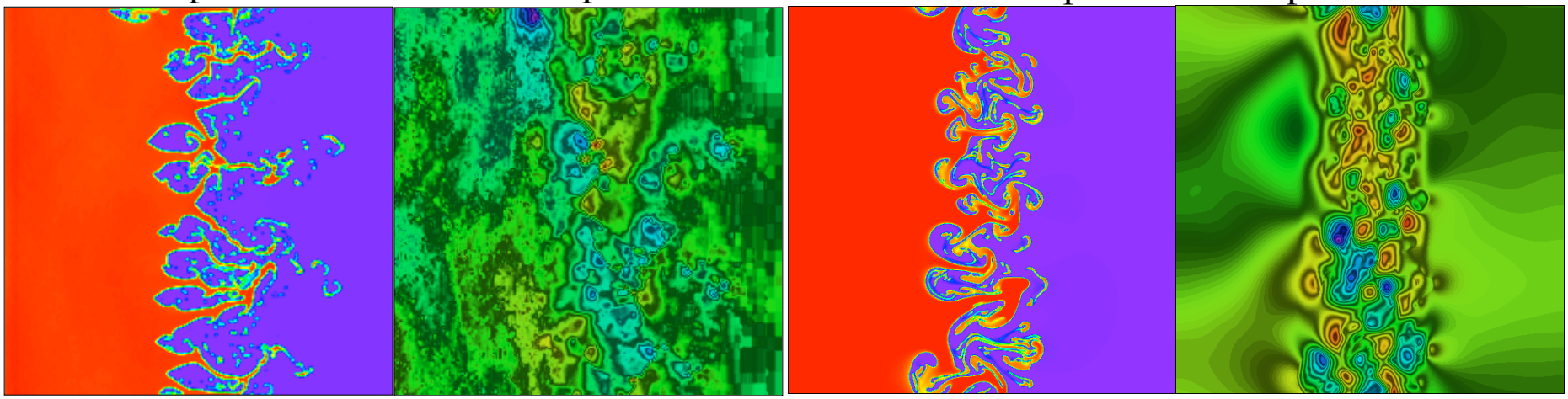

density | pressure perturbation | density | pressure perturbation

applied physics division

Los Alamos NATIONAL LABORATORY

E.L.Vold

R-T compressibility issues: Epilogue

- This is a collection of view graphs (LA-UR-04-4778) as presented at the IWPCTM9, Cambridge, UK, July19-23, 2004, intended to promote discussion.
- A more formal write-up is planned.
- Technical issues which have been discussed since this work was presented are summarized briefly here:
  - There are significant qualitative and quantitative differences between the pressure fluctuations seen here in the fully multi-fluid compressible formulation and in some incompressible formulations.
    - Pressure fluctuations are localized within the mix layer in incompressible calculations while they propagate as waves throughout the domain (more realistically it is believed) in the multi-fluid compressible calculations.
    - Internal energy fluctuations are seen to be a major contributor to pressure fluctuations here, while in an incompressible calculation there are no internal energy fluctuations.
    - Compressibility terms in the density and the energy equations are significant in the average mix layer profiles compared to the incompressible advection terms.
  - It is hypothesized these differences may be important in understanding the widely reported difference [e.g., see Dimonte, et.al., IWPCTM8] between R-T growth rates in experiment and in many codes as, $\alpha_{exp} \sim 0.05 - 0.075$ and $\alpha_{calc} \sim 0.03 - 0.04$.
    - It is implied that some 'compressible computations' with an averaged internal energy may behave more like incompressible than compressible fluids, underestimating the fluctuation levels and thus underestimating the effective growth rates. Mix growth rates in a mode-coupling limit [Dimonte, et.al.,Phys.Fluids, v.(),p.2004] may not be fully representing the fluctuation modes in real experiments.
    - It is implied that the experiments will exhibit compressible fluid properties regarding the fluctuations, even though the regime is considered in the 'incompressible limit'.
    - A true multi-fluid formulation (with complete thermodynamic properties for two distinct fluids at the interface) appears in some previous calculations, (e.g., in the 'Frontier code' of Glimm, et.al.), and they report higher alpha values, in agreement with the present study and with most experiments.

E.L. Vold

Compressible aspects in simulations of multi-mode Rayleigh-Taylor mixing

Abstract

LA-UR-04-0243

Presentation to the IWPCTM9
Cambridge, UK, July 19-23, 2004

Compressible aspects of the Rayleigh-Taylor mixing layer are explored in 2-D (x-y) multi-mode IC resolved scale simulations solving the multi-fluid Euler equations with interface reconstruction. R-T mix layer growth rates are computed in an 'incompressible limit' and found to be in agreement with experimental data across the range of Atwood numbers (0.04-0.96) for bubbles and for spikes. Fluctuation contributions to mixing are examined in contour plots, profiles of transverse averaged quantities, and in spectra of pressure and pressure components, momentum components, and the advection and compressible terms in the density and energy equations.

Results show pressure fluctuations are driven by density fluctuations with a comparable contribution from the energy fluctuations omitted in incompressible formulations. Transverse planar averaged magnitudes of fluctuations for density over that for internal energy are less than unity in the bubble growth region and greater than unity in the spike growth region, implying fluctuations are dominated by different contributions in each region. The magnitudes of compressible terms compared to the incompressible advection terms in the density and in the energy equations show significant trends averaged across the mix layer. Compressible contributions to fluctuations are most important for density in the bubble growth region and for internal energy in the spike growth region. Long wave length modes in the initial conditions, which have been proposed by others as a mechanism for enhanced mix layer growth rates, are seen to be inescapable in the present multi-fluid compressible formulation. Vorticity and other fluctuating components play key roles in dissipating the instability acceleration into the transverse plane and thus establishing the characteristic gradient scale lengths across the mix layer and the effective mix layer growth rates within each fluid region.

The results together show that density and internal energy fluctuations, including the compressibility terms, are significant contributions to the dynamics. This supports the concept that mix layer growth is driven by interface physics which depends upon discontinuities in both density and in internal energy. It is hypothesized that this physics must be properly represented in a multi-fluid simulation in order to match multi-mode growth rates in experiments even in the 'incompressible limit'.

applied physics division

Los Alamos NATIONAL LABORATORY

"Compressible aspects in simulations of multi-mode Rayleigh-Taylor mixing" E.L.Vold

Topics

- Introduction
  - R-T multimode growth rates, h = αAgt^2
    - $\alpha_{computed} < \alpha_{experimental}$ => may be compressibility
  - Methods: compressible vs. incompressible (thermodynamic p vs. dynamic p)
    - compressible P[ρ,e] => pressure coupled to 2 wave equations {for ρ and e}
    - incompressible P[div*u=0] => Poisson equation w/ source: $\nabla \cdot [u \cdot \nabla u]$
- Results: Fluctuation Quantities
  - Gallery of fluctuation quantities, p, u, v, E, ρ, $\nabla \cdot u$, etc….
  - FFT components in: $\Delta p = (\gamma - 1)\Delta\rho\Delta\varepsilon + (\gamma - 1)\rho\Delta\Delta\varepsilon$
  - Mix layer profile averages of: $\langle | u \cdot \nabla \rho | \rangle$, $\langle | u \cdot \nabla e | \rangle$, $\langle | \rho \nabla \cdot u | \rangle$, $\langle | e \rho \cdot u | \rangle$
- Results: Pressure Gradient Fields
  - Dp/dz distributions
  - Dp/dz compressible compared to incompressible
- Summary: consistent picture of role of compressibility in R-T multi-mode mix layer growth rates.

Pressure fluctuation field Compressible (left) vs incompressible (rt)

E.L.Vold

density

Thermodynamic pressure, p[ρ,e]: source in fluctuating densities and internal energy.

Dynamic pressure potential, p[u]: source in mix region where u.ne.0.

density

$\nabla p = (\gamma - 1)\nabla\rho\,\nabla e + (\gamma - 1)\rho\,\nabla^2 e$

$\nabla \cdot (\rho^{-1}\nabla p) = \nabla \cdot (u \cdot \nabla u + \rho\,\nabla^2 u)$

$p_{src}[\nabla \cdot u => 0]$

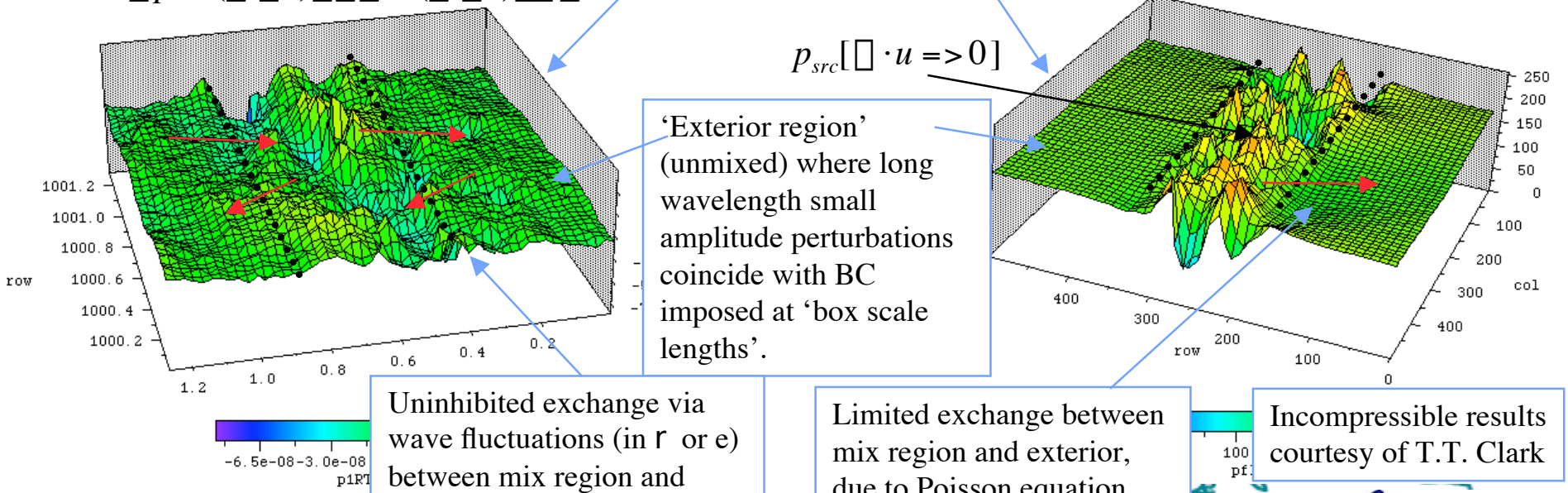

'Exterior region' (unmixed) where long wavelength small amplitude perturbations coincide with BC imposed at 'box scale lengths'.

Uninhibited exchange via wave fluctuations (in ρ or e) between mix region and exterior region long wavelength perturbations.

Limited exchange between mix region and exterior, due to Poisson equation for kinetic potential pressure, p

Incompressible results courtesy of T.T. Clark

applied physics division

Los Alamos NATIONAL LABORATORY

R-T study summary

E.L. Vold

- R-T instability is: $a(t) = a_o$ compared to "R-T" instability, $\nabla p(t) \cdot \nabla \rho(t) < 0$
- Methods:
  - Resolved scale Euler equation simulations of Rayleigh instability from hydrostatic equilibrium w/ IC multi-mode perturbations, $\eta_o \sim$ Vf +/- 0.02-0.1, $l_o \sim 10$ - 50 dx, $k_o \sim 12$ - 50 across 2-D grids of 128^2, 256^2 and 512^2.
  - Compressible multi-fluid methods set to low compressibility w/ and w/o Interface Reconstruction (IR).
  - Range of Atwood numbers examined from 0.96 to 0.04, base case studies at A=0.8.
- Results:
  - Alpha bubble (~ 0.055-0.06) and alpha spike in good agreement with experiments across all Atwood numbers.
  - Allowing numerical diffusion (Interface Reconstruction -IR- off) has a small effect: pulls alpha-bub and alpha-spike closer together (increases alpha-bubble slightly) implying numerical diffusion may not be limiting the correct alpha.
  - Vorticity and compressibility roles are important in density and energy fluctuations.
- Conclusions:
  - Code results for resolved scale wavelengths from sub-grid IC amplitudes appear to be valid.
  - Multi-fluid compressibility is a likely source of agreement with experiments.

E.L. Vold

Issues in R-T mix

- Multi-mode growth rate as: $h = \alpha A g t^2$
  - $\alpha_{experimental} \sim 0.05 - 0.07 > \alpha_{computed} \sim 0.04$ (some calcs up to ~ 0.07)
  - Many computations are incompressible or 'averaged compressible single fluid'.
- Pressure is a thermodynamic quantity in real fluids.
  - Incompressible pressure is dynamic p[div*u] with a significant source only in the mix layer. Long wave growth is limited.
  - Compressible pressure is thermodynamic and fluctuations within mix layer exchange energy with fluctuations beyond mix width through 'acoustic oscillations'.
- Pressure fluctuations are driven by density and internal energy fluctuations.
  - Incompressible calculation has no energy fluctuations, and single fluid compressible formulation can yield no 'new fluctuation information'.
  - Multi-fluid energy fluctuations are distinct from density fluctuations and contribute to pressure fluctuations driving mix.

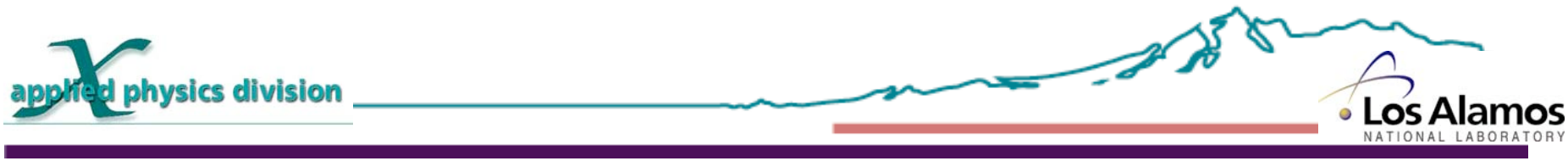

E.L.Vold

Summary of Relevant Work

- **Experimental**
  - wide range of experiments (mostly incompressible) show a mix layer growth rate which closely approximates the scaling, $h = \alpha A_t g t^2$
  - alpha bubble,
    - α_b ~ 0.06-0.07 (earlier work, e.g., Youngs and Read et.al.,)
    - ~ 0.05 (recent work, e.g., Dimonte, Schneider, et.al.)
  - alpha bubble and alpha spike
    - variations w/ Atwood number ==>>

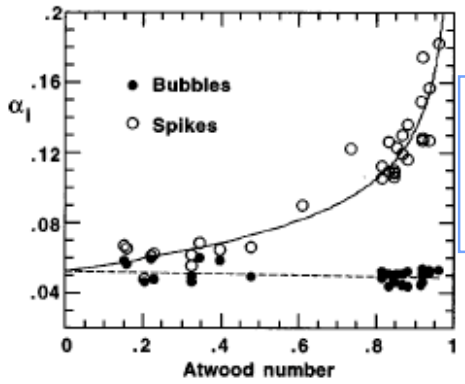

reference: G.Dimonte, Phys.Plasmas,6(5), 2009 (1999).

- **Computational**
  - alpha bubble results range from ~ 0.03 - ~ 0.08
  - many 3-D methods (compressible or incompressible) trending towards low end, α_b ~ 0.03 ~ half experimental mean
  - front tracking w/ 2 distinct fluids ('Frontier code', Glimm, et.al.) at higher end, ~0.07-0.08
  - large variance in alpha just due to random seed in initial perturbation
    - (~ 0.05 +/- 20-50%, in 2-D compressible isothermal fluids, T. Clark, 2001)
  - 2-D results ~ 15% greater than 3-D results (Youngs, 1994).

E.L.Vold

Summary of The Methods

- Methods
  - 2-D (x-y or r-z) multi-fluid Eulerian formulation
    - each fluid has its own density, internal energy and pressure in its fluid volume fraction within the 'mixed cells' (containing the interface)
  - compressible Euler equations in appropriate limit to recover incompressible approximation, supplemented with fluid volume fractions
  - ideal gas equation of state for each fluid
  - advection of fluid volume fractions in mixed cells at the interface
    - mixed cell treatment (Bowers and Wilson,1991)
    - interface reconstruction (D.Youngs, 1984, 1989)
  - high-order, monotonic Van Leer advection of fluid quantities
  - AMR (adaptive mesh refinement) used to improve efficiency of calculation
    - Introduces negligible contributions to pressure fluctuations
  - IC hydrostatic equilibrium set-up uses constant densities with linear internal energy profiles
    - Same results (RT mix growth rates) for constant energy, variable density IC

E.L.Vold

Fluid Equation Forms

$$\rho = \rho_1 + \rho_2 = Vf_1\rho_{s\,1} + Vf_2\rho_{s\,2} = Vf_1\rho_{s\,1} + (1 - Vf_1)\rho_{s\,2}$$

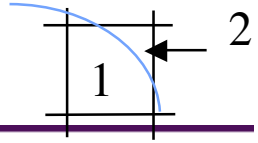

Incompressible w/ V_f or m_f = f[r]

$$\frac{\partial \rho}{\partial t} + \nabla \cdot \rho u = 0$$

$$\frac{\partial u}{\partial t} + u \cdot \nabla u + \frac{\nabla p}{\rho} = 0$$

$$\nabla \cdot u = 0$$

$$\nabla \cdot \left(\rho^{-1} \nabla p\right) = -\nabla \cdot (u \cdot \nabla u)$$

Solution =f[ρ,p,u**]**

Compressible inviscid (Euler) w/ V_f or mass fraction, m_f

$$\frac{\partial m_f \rho}{\partial t} + \nabla \cdot m_f \rho u = 0$$

$$\frac{\partial \rho}{\partial t} + \nabla \cdot \rho u = 0$$

$$\frac{\partial u}{\partial t} + u \cdot \nabla u + \frac{\nabla p}{\rho} = 0$$

$$\frac{\partial \rho e}{\partial t} + \nabla \cdot \rho e\, u = -p \nabla \cdot u$$

$$p \overset{idealEOS}{=} T_0 R \rho = P_0 \rho$$

$$(\gamma_{eff}[m_f, M_1, M_2, Cv_1, Cv_2] - 1)\rho e$$

Solution =f[ρ,e,m_f,p,u**]**

Two-fluid, inviscid, single velocity, compressible forms

$$\frac{\partial V_f}{\partial t} + u \cdot \nabla V_f = 0 \quad **$$

2x: $$\frac{\partial \rho_i}{\partial t} + \nabla \cdot \rho_i u = 0$$

$$\frac{\partial u}{\partial t} + u \cdot \nabla u + \frac{\nabla p}{\rho} = 0$$

2x: $$\frac{\partial \rho e_i}{\partial t} + \nabla \cdot \rho e_i u = -p_i \nabla \cdot u$$

$$p = p_1 + p_2 = Vf_1 p_{s\,1} + Vf_2 p_{s\,2} \overset{idealEOS}{=} Vf_1(\gamma_1 - 1)\rho_{s\,1} e_{s\,1} + Vf_2(\gamma_2 - 1)\rho_{s\,2} e_{s\,2}$$

Solution =f[ρ_1,ρ_2,e_1,e_2,V_f,p,u**]**

** sensitive to implementation detail

$$\frac{\partial V_f}{\partial t} + \nabla \cdot V_f u = 0$$

$$\frac{\partial V_f}{\partial t} + u \cdot \nabla V_f = -V_f \nabla \cdot u \neq 0$$

Incompressible implies ==>>

$$\nabla \cdot u = 0$$

$$\rho_{si} = const \Rightarrow \frac{\partial \rho_{si}}{\partial t} = 0 \Rightarrow \nabla \rho_{si} = 0$$

$$e_i = const \Rightarrow \frac{\partial e_i}{\partial t} = 0 \Rightarrow \nabla e_i = 0$$

applied physics division

Los Alamos NATIONAL LABORATORY

E.L. Vold

Implications of different equation sets

Incompressible dynamic pressure:

At the IC interface in an incompressible set-up, density discontinuity exists with pressure continuity, and pressure is a dynamic quantity, p ~ f(u).

$$\nabla \cdot \left(\rho^{-1} \nabla p\right) = \nabla\nabla \cdot \left(u \cdot \nabla u\right)$$

and coupled to: $\dfrac{\partial u}{\partial t} + u \cdot \nabla u + \dfrac{\nabla p}{\rho} = 0$ $\qquad \dfrac{\partial \rho_i}{\partial t} + \nabla \cdot \rho_i u = 0$

Compressible thermodynamic pressure:

At the IC interface in a compressible set-up, density discontinuity and internal energy discontinuity are consistent with pressure continuity (constant g). The density and energy discontinuities each act as a source to make separate contributions to p', as p=(ρ,e) is a thermodynamic quantity.

$$\nabla \cdot (\rho^{-1} \nabla p) = \nabla \frac{\partial \rho \cdot u}{\partial t} \nabla\nabla \cdot [u \cdot \nabla u]$$

coupled thru: $\dfrac{\partial \rho \cdot u}{\partial t} = \dfrac{\ddot{\rho} V}{V} = f[\ddot{\rho}, \ddot{e}]$

V = a fluid element volume

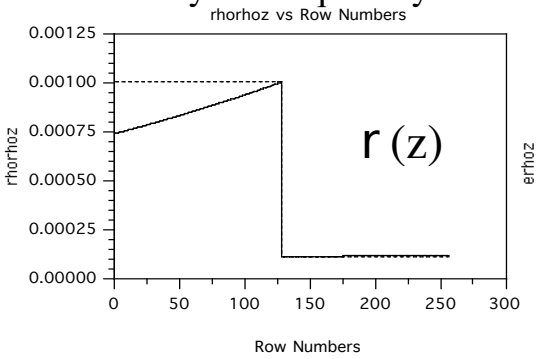

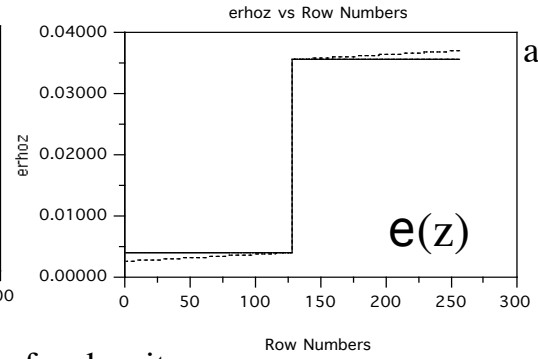

and coupled to: $\dfrac{\partial \rho_i}{\partial t} + \nabla \cdot \rho_i u = 0$

$$\frac{\partial \rho e_i}{\partial t} + \nabla \cdot \rho e_i u = \nabla p_i \nabla \cdot u$$

and finally back to:

$$p = p_1 + p_2 = Vf_1 p_{s\,1} + Vf_2 p_{s\,2} \quad \text{idealEOS}$$

$$Vf_1(\rho_1 \nabla 1)\nabla_{s\,1} e_{s\,1} + Vf_2(\rho_2 \nabla 1)\nabla_{s\,2} e_{s\,2}$$

or as wave equations for density or energy:

$$(\ddot{\rho} + D_\rho \dot{\rho})/\rho \sim f_p \nabla^2 \rho + \frac{e}{\rho} \nabla^2 e \qquad (\ddot{e} + D_\rho \dot{e})/e \sim f_p \nabla^2 \rho + \frac{e}{\rho} \nabla^2 e$$

or:

applied physics division

Los Alamos NATIONAL LABORATORY

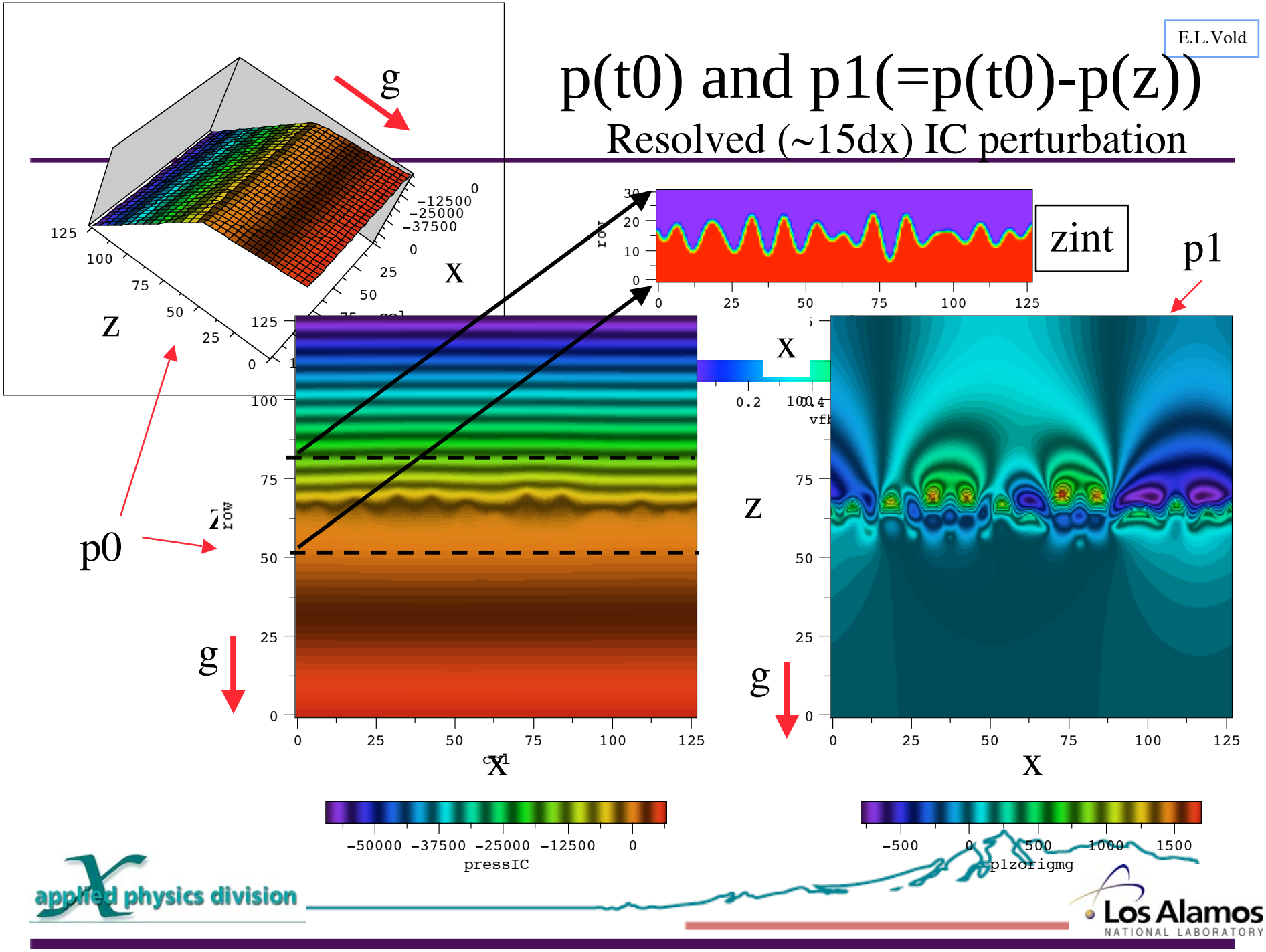
E.L.Vold
p(t0) and p1(=p(t0)-p(z))
Resolved (~15dx) IC perturbation
g
z
x
zint
p1
p0
pressIC
p1zorigmg
applied physics division
Los Alamos
NATIONAL LABORATORY

E.L. Vold

Initial Conditions for density and pressure perturbation (p1 = p - $\langle p \rangle_y$) for resolved vs. unresolved IC interface

Resolved IC: initial perturbation amplitude varies over several zones and volume fraction varies in a single zone at the interface. IC pressure field varies significantly to the boundary.

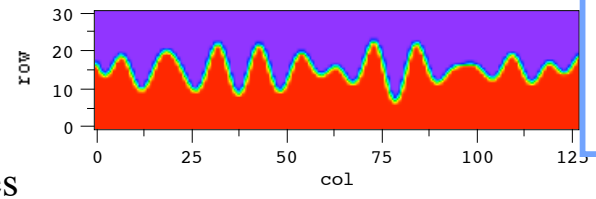

This set-up was used in all cases reported here

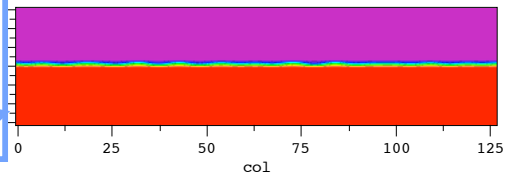

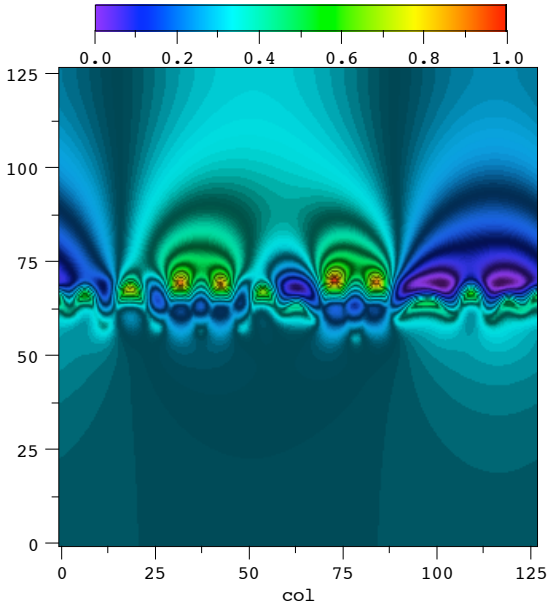

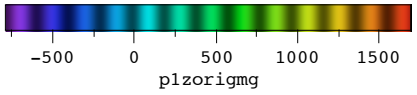

Un-resolved IC: initial perturbation amplitude (for same IC modal structure shown in previous case) varies as the volume fraction in a single zone at the interface. IC pressure field is rapidly attenuated away from the interface.

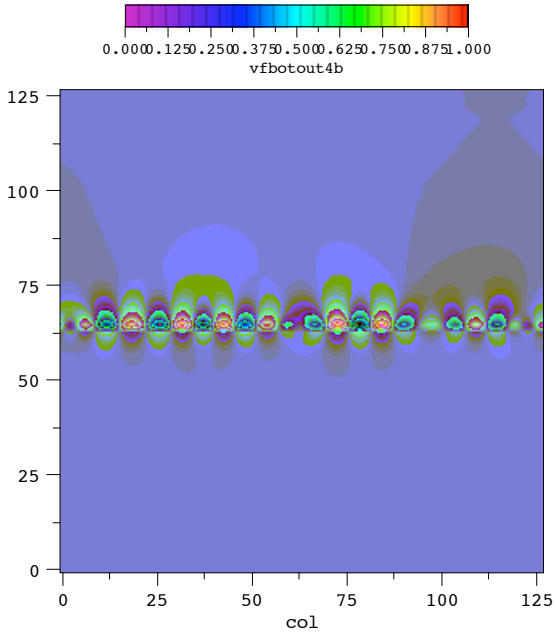

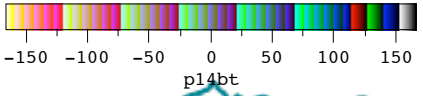

applied physics division

Los Alamos NATIONAL LABORATORY

E.L.Vold

R-T equilibrium IC for r (z) or e(z)

(either IC led to nearly identical results in mix layer growth)

IC Equilibrium:

$$\nabla p = \rho g$$

For constant internal energy:

$$\rho(z) = \rho_o e^{z/L}$$

ideal gas $\rho_o e^{zg/(\gamma-1)\theta}$

For constant density:

$$\rho(z) = \rho_o + \rho' z$$

ideal gas $\rho_o + \frac{g}{(\gamma-1)\theta} z$

For either case:

$$\nabla p(z) / \rho(z) = g$$

$\rho_1 = \rho_2$

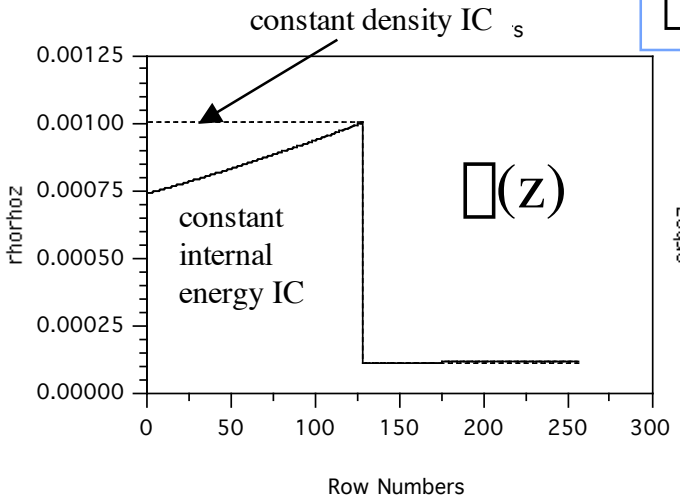

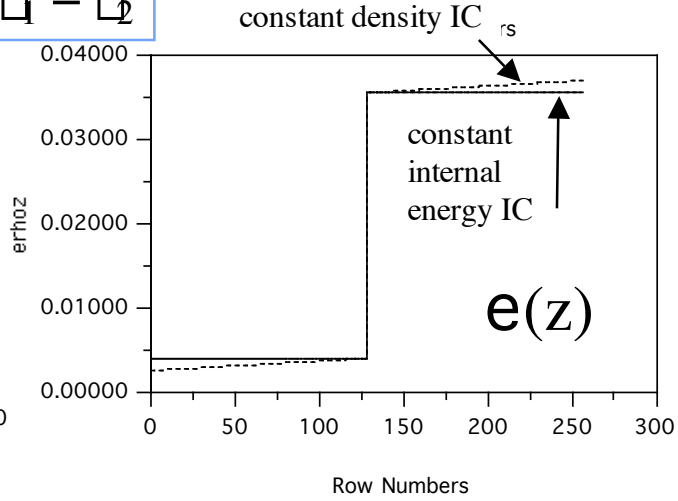

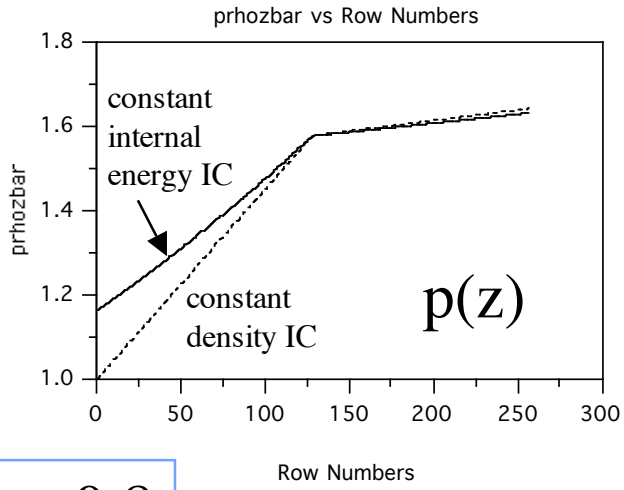

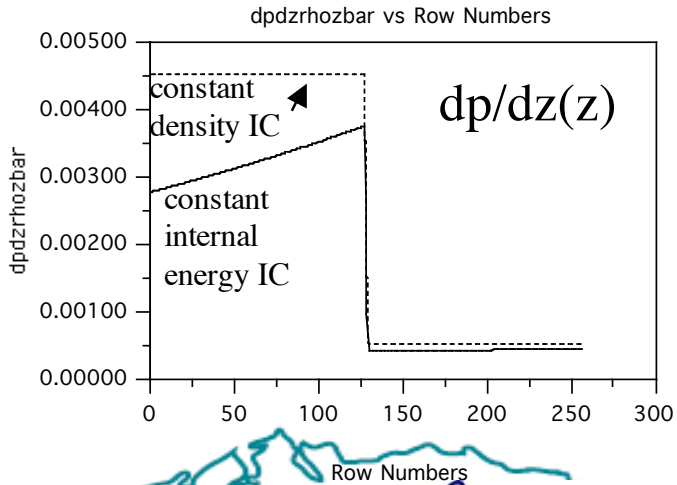

Atw=0.8

E.L.Vold

Density and pressure contours, pressure axial(x) profile and dpdx(x) at an early time and a late time**

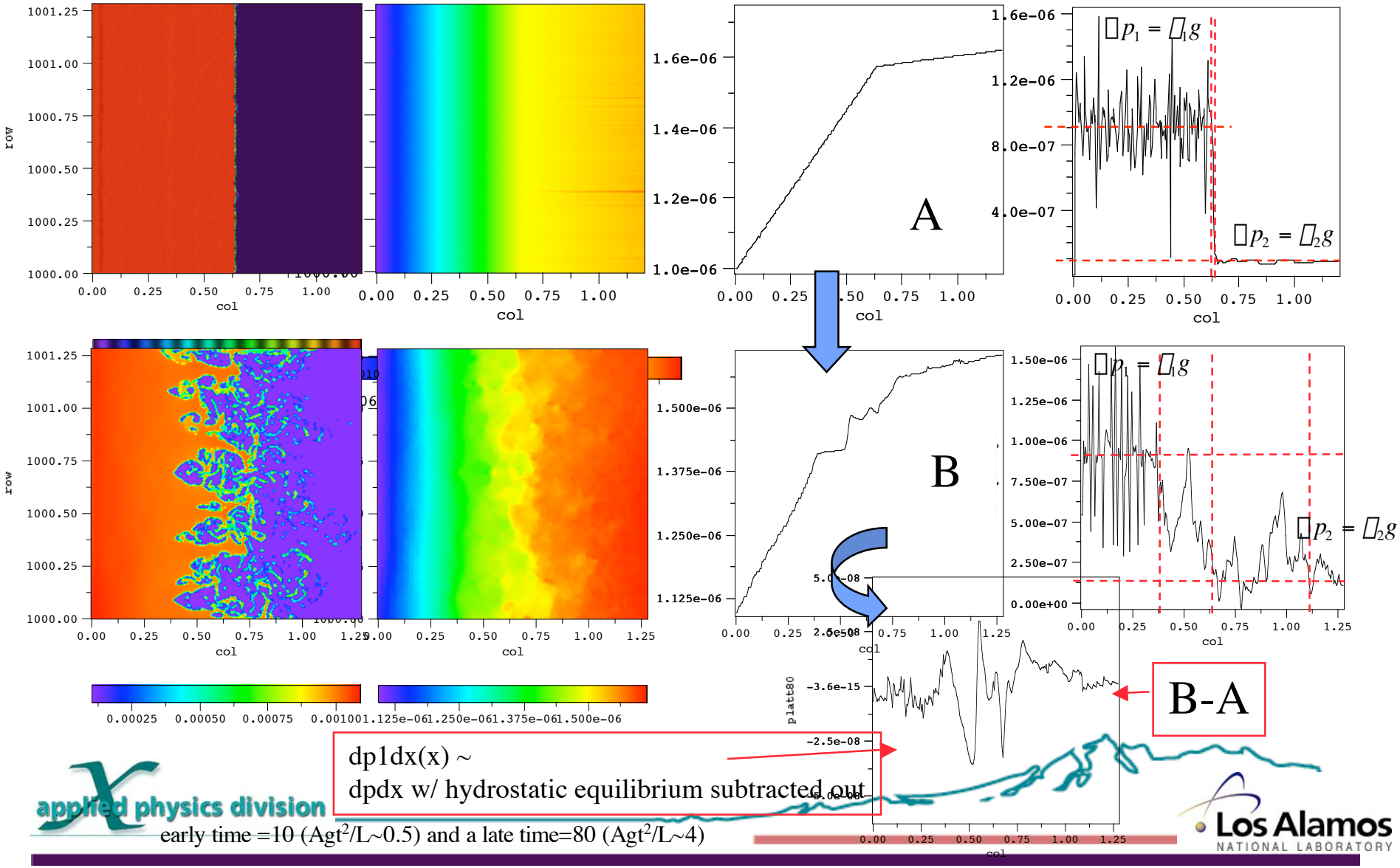

dp1dx(x) ~
dpdx w/ hydrostatic equilibrium subtracted out

early time =10 (Agt^2/L~0.5) and a late time=80 (Agt^2/L~4)

E.L.Vold

pressure profile for varying compressibility

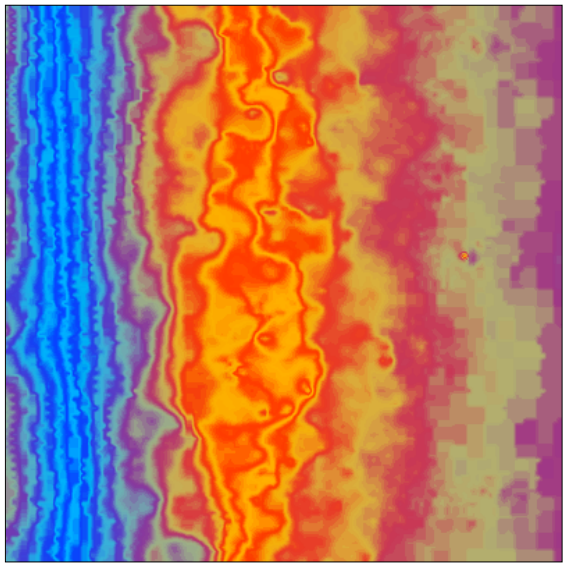

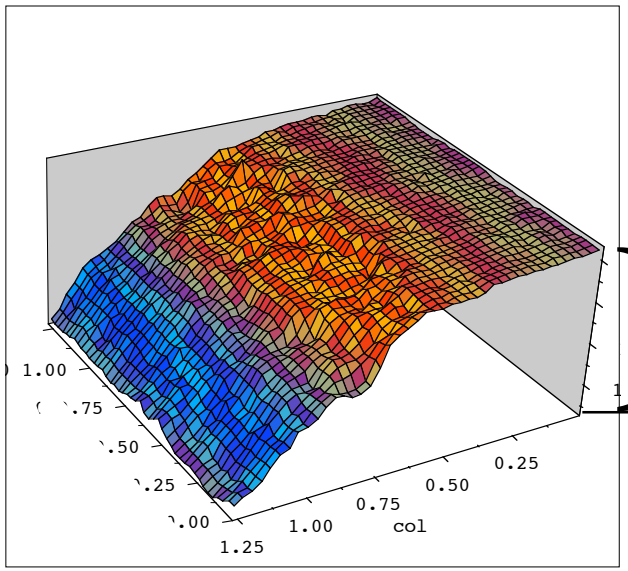

ideal gas EOS:
$P = (\gamma - 1)\rho e_{in}$

hydrostatic equilibrium:

$$\nabla p \sim \frac{dP}{L} = \rho g$$

dP

P_{min}

(in)compressibility varied by increasing P_{min} thru e_{in} (~T),
while maintaining same pressure gradient and hydrostatic equilibrium

higher e_{in} ==>> Cs $^{1/2}$

applied physics division

Los Alamos NATIONAL LABORATORY

E.L. Vold

RT mix at t=60 for varying compressibility

dp/dz, ρ and g maintained constant, and p increased (increasing Cs*) for increased incompressibility

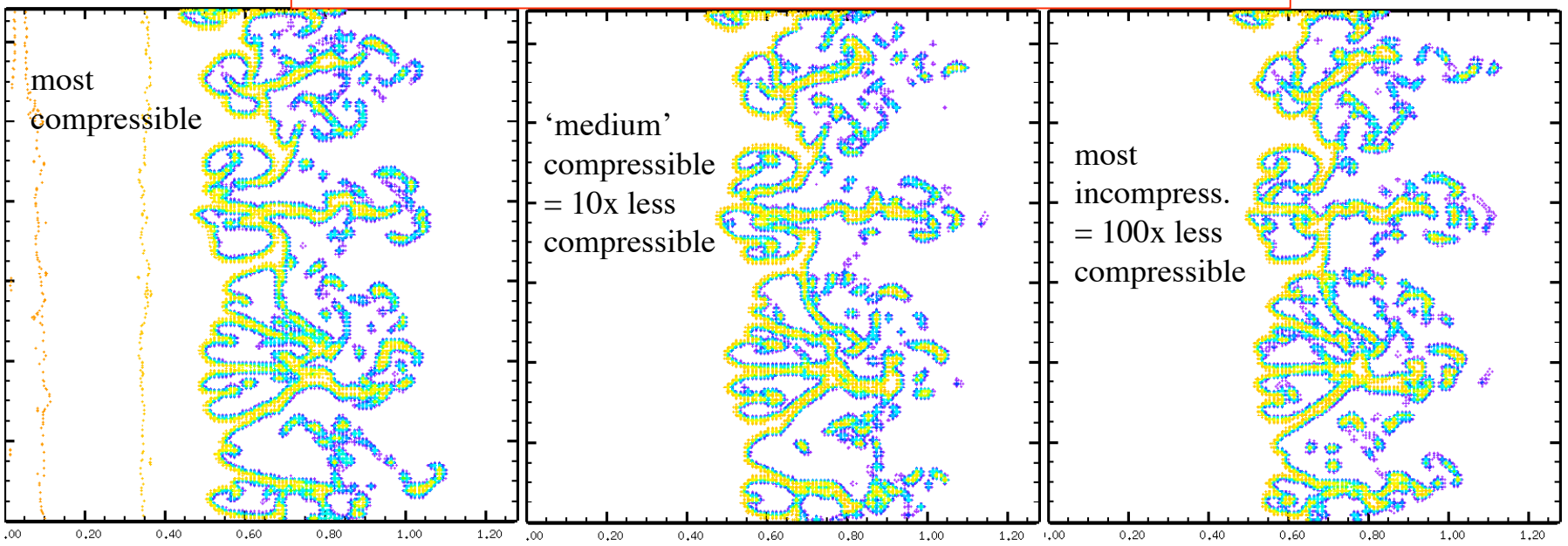

b7r (dp/p~0.3) cycle=1775 c11 (dp/p~0.03) cycle=4475 c21 (dp/p~0.003) cycle=13650

$Ma^2 \sim 0.01$

* increasing p by 10 => Cs increases ~ $10^{1/2}$ ~ 3, so dt decreases and number of cycles up ~ 3x per panel

applied physics division

Los Alamos NATIONAL LABORATORY

E.L. Vold

RT mix at late time -varying Atwood number

At = 0.96
□1/□2 = 50
t = 60 (z = 2.6)

At = 0.8
□1/□2 = 9
t = 80 (z = 3.84)

At = 0.33
□1/□2 = 2
t = 120 (z = 3.6)

At = 0.048
□1/□2 = 1.1
t = 320 (z = 3.66)

Density

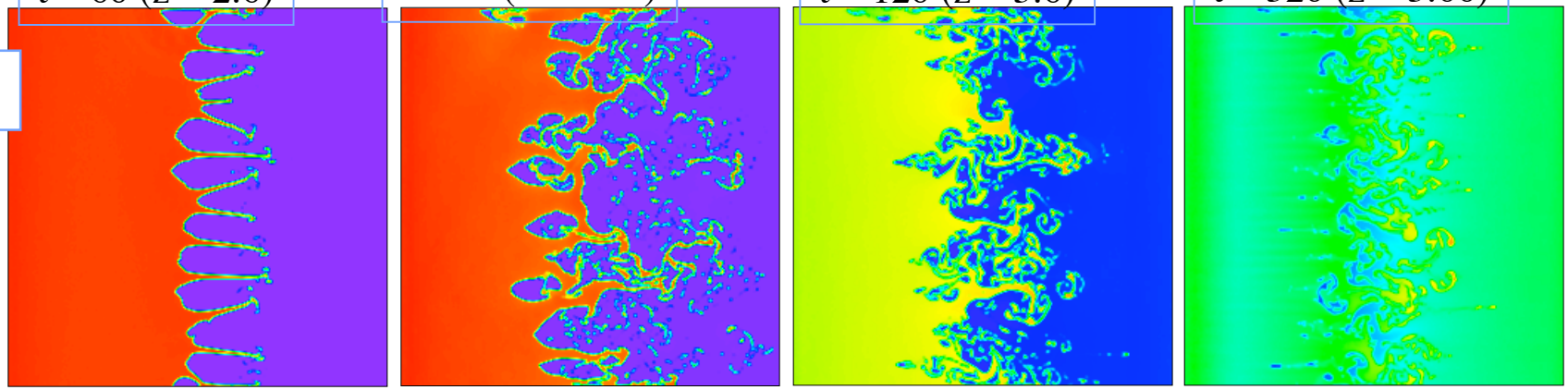

P1 = Pressure Fluctuations

P1= $p(x,y) - \langle p(x,y) \rangle_y$ (w/o hydrostatic pressure)

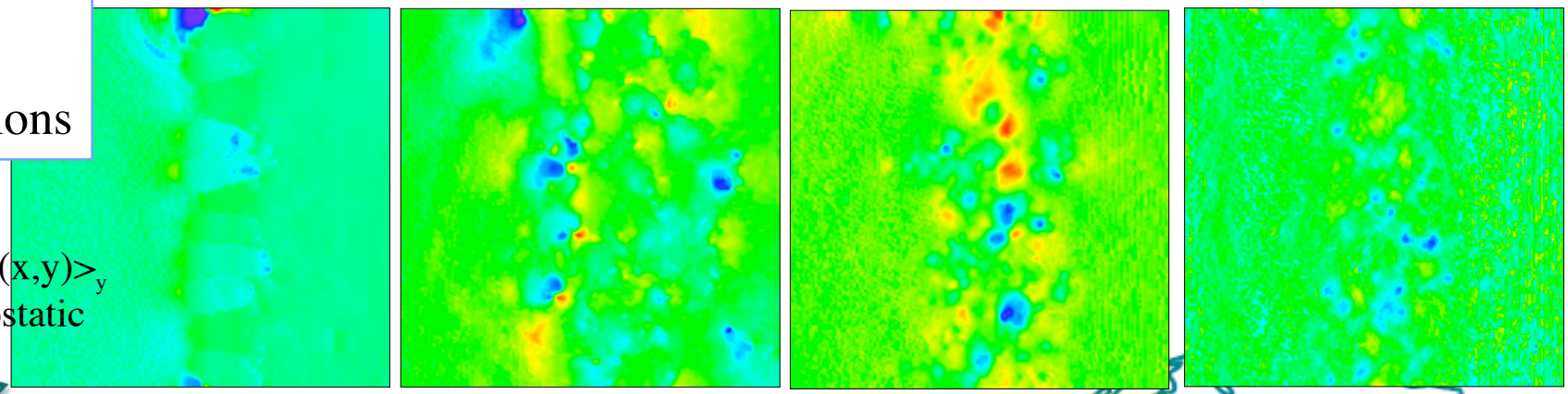

applied physics division

Los Alamos NATIONAL LABORATORY

RT growth rates: alpha bubble and spike vs. Atwood number - Calc. & Exper.-

E.L.Vold

Calculations w/IR
(w/ interface reconstruction)

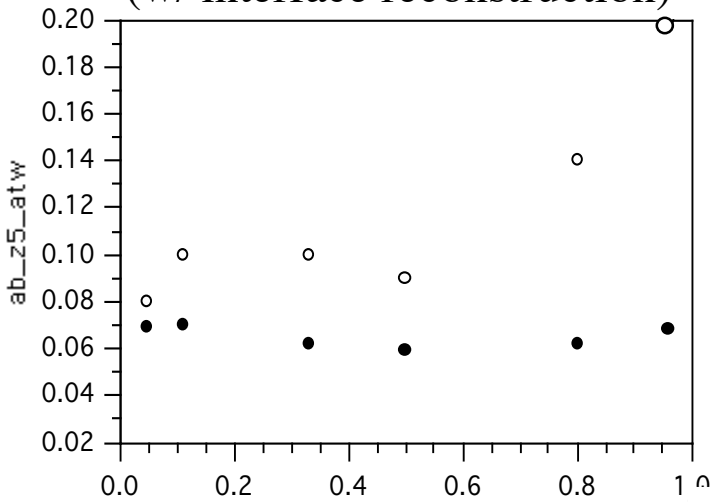

Calculations show trends in agreement with experiment, with computed alphas slightly higher than in this set of experiments.

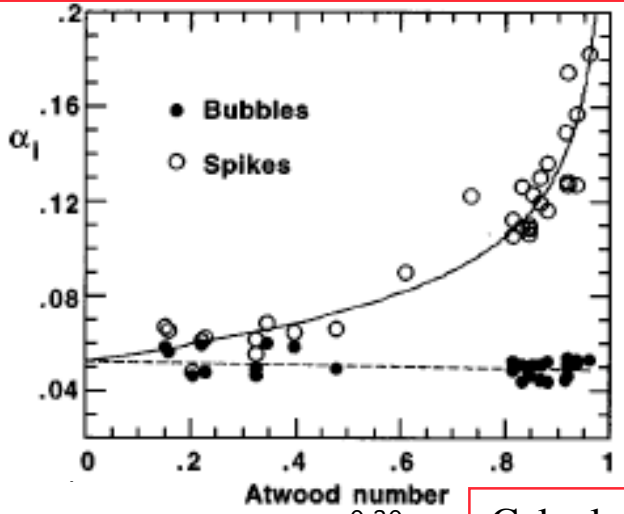

Experimental Results - Figure from Dimonte, et.al. 1998)

Calcs with IR compared to calcs without IR

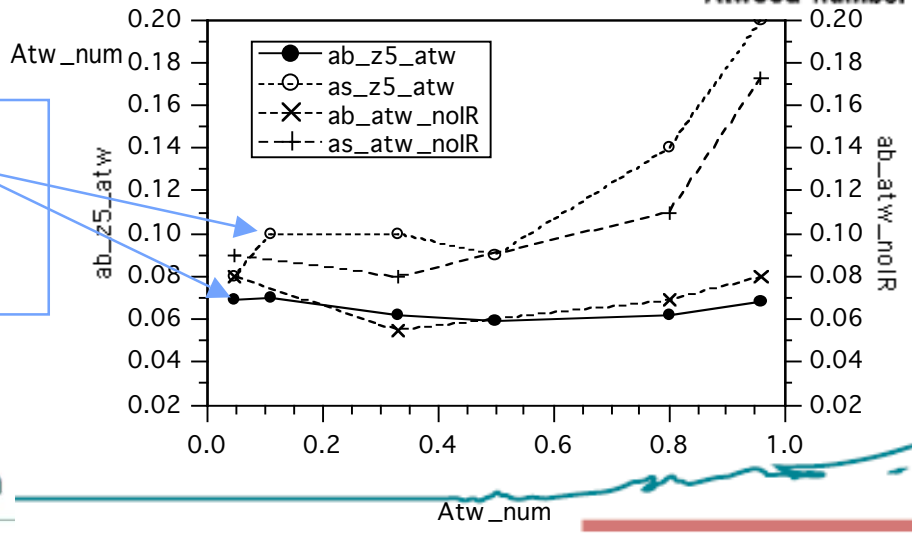

Calculations with IR & without IR are similar- Suggests that interface treatment is not critical to growth rate - Multi-fluid treatment is proposed

applied physics division

Los Alamos NATIONAL LABORATORY

Multi-fluid equations and important terms in compressible R-T mixing RESULTS

E.L.Vold

Multi-fluid equations general form:

$$\frac{\partial \rho_i}{\partial t} + \nabla \cdot \rho_i u = 0$$

$$\frac{\partial u}{\partial t} + u \cdot \nabla u + \frac{\nabla p}{\rho} = 0$$

$$\frac{\partial \rho e_i}{\partial t} + \nabla \cdot \rho e_i u = -p_i \nabla \cdot u$$

$$p = p_1 + p_2 = Vf_1 p_{s1} + Vf_2 p_{s2} \quad \text{idealEOS}$$

$$Vf_1(\gamma_1 - 1)\rho_{s1} e_{s1} + Vf_2(\gamma_2 - 1)\rho_{s2} e_{s2}$$

$$\frac{\partial V_f}{\partial t} + u \cdot \nabla V_f = 0$$

Multi-fluid equation terms shown in R-T profile plots:

$$\frac{\partial \rho_i}{\partial t} + u \cdot \nabla \rho_i = -\rho_i \nabla \cdot u$$

$$\frac{\partial e_i}{\partial t} + u \cdot \nabla e_i = -\frac{p_i}{\rho_i} \nabla \cdot u = -(\gamma_i - 1) e_i \nabla \cdot u$$

$$\rho \left(\frac{\partial u}{\partial t} + u \cdot \nabla u \right) + \nabla p = 0$$

$$p \quad \text{idealEOS} \quad \rho[(\gamma - 1)e] = \text{const} \quad (\gamma - 1)[\rho e + e\rho]$$

pressure gradient component terms:

w/ equilibrium and fluctuation contributions:

(our case) $\rho e = \rho e_o + \rho e_1$ (or) $\rho = \rho_o + \rho_1$

RESULTS in following Vus:

- Spectra for contributions to pressure fluctuations (data in transverse y direction at location of interface in IC).
- Contours of fluctuating quantities in the mix layers.
- Profile averages of fluctuation quantities through the mix layer
- Pressure gradient terms in the compressible simulations.
- Pressure gradient terms compared: compressible vs. incompressible simulations.

E.L.Vold

Spectral densities (Fourier mode amplitudes) for density, internal energy by times, t = 0, 10, 40, 80

t = 0 ($z=Agt^2 = 0$)

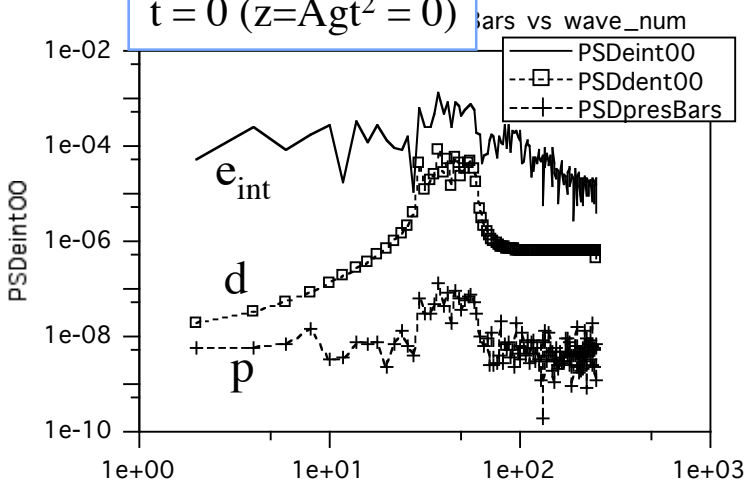

t = 10 ($z=Agt^2 \sim 1/2$)

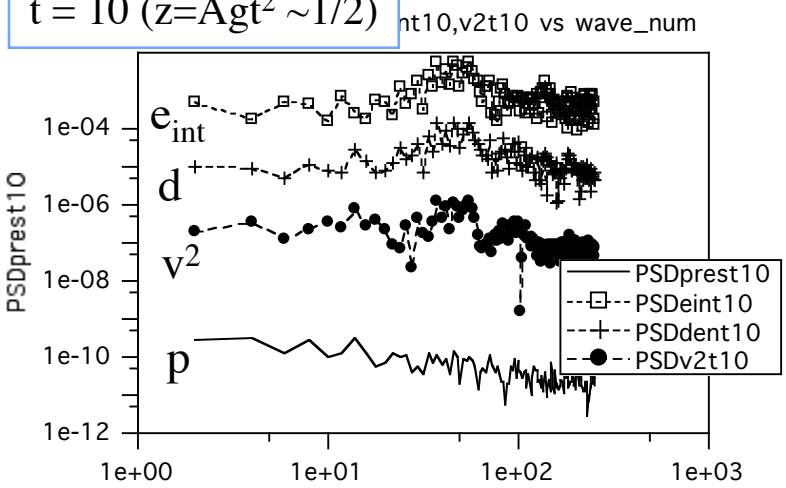

wave_no -k-

t = 40 ($z=Agt^2 \sim 1$)

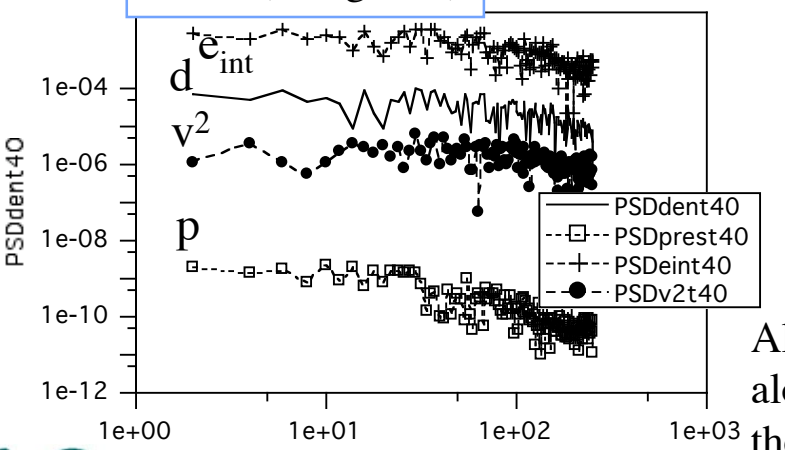

t = 80 ($z=Agt^2 \sim 4$)

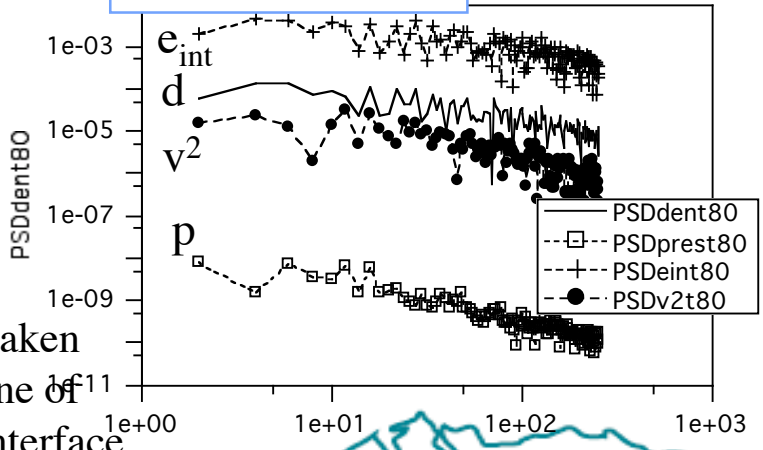

wave_no -k-

wave_no -k-

wave_no -k-

All data is taken along the line of the initial interface location, z = 0.

Vold

Estimating transverse pressure fluctuation contributions at late time (t=80) from spectral coefficients for density, internal energy and pressure, transversing the R-T mix layer

momentum equation

$$\frac{\partial u}{\partial t} + u \cdot \nabla u + \frac{\nabla p}{\rho} = g$$

with ideal gas EOS

$$p = (\gamma - 1)\rho\varepsilon$$

linearize p as function of density and internal energy

$$\frac{\partial u}{\partial t} + u \cdot \nabla u \approx \frac{(\gamma - 1)}{\rho_o}(\rho_o \nabla \varepsilon + \varepsilon_o \nabla \rho)$$

grad(p) as f[density and energy spectral coefficients]

$$= (\gamma - 1)\left[\nabla \rho + \frac{\rho_o \nabla \varepsilon}{\varepsilon_o}\right] = (\gamma - 1)\left[\nabla \rho + \frac{p_o \nabla \rho}{\rho_o^2}\right] \sim (\gamma - 1)\left[k_{max} f_{max}(\rho) + \frac{\rho_o k_{max} f_{max}(\varepsilon)}{\varepsilon_o}\right]$$

$$\left(\frac{\rho_o}{\rho_o}\right)_{heavy\ fluid} \sim \frac{0.004}{0.001} \sim 4$$

$$\left(\frac{\rho_o}{\rho_o}\right)_{light\ fluid} \sim \frac{0.035}{0.000111} \sim 320$$

$$\left(\frac{\nabla p}{\rho}\right)_{heavy\ fluid} \sim (\gamma - 1)\nabla \rho$$

$$\left(\frac{\nabla p}{\rho}\right)_{light\ fluid} \sim (\gamma - 1)\frac{\rho_o}{\varepsilon_o}\nabla \varepsilon$$

$$\left(\frac{\rho_o}{\rho_o}\right)_{light\ fluid} \Big/ \left(\frac{\rho_o}{\rho_o}\right)_{heavy\ fluid} \sim \left(\frac{p_o}{\rho_o^2}\right)_{light\ fluid} \Big/ \left(\frac{p_o}{\rho_o^2}\right)_{heavy\ fluid} \sim 80$$

$f_{max}(e) \sim 4e\text{-}3$

$f_{max}(r) \sim 1e\text{-}4$

Spectral coefficients from transverse profiles at z=0.

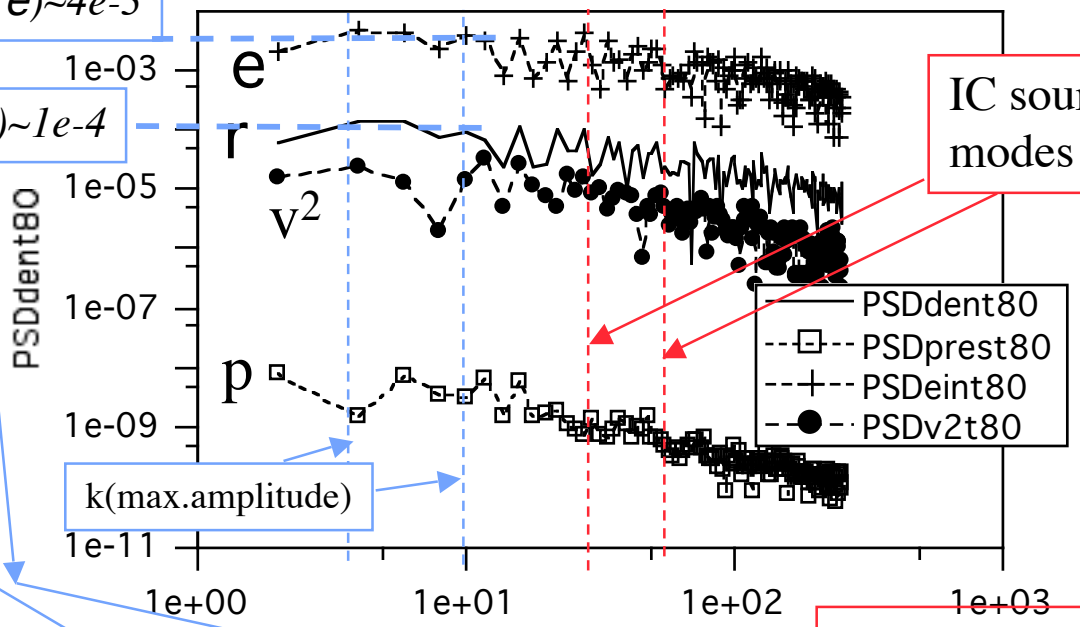

IC source modes

Ergo: Pressure fluctuations driven by e in heavy fluid and by r in light fluid.

applied physics division

Los Alamos NATIONAL LABORATORY

E.L. Vold

FFTs p-t80 128 & 512

p spectra (left) w/ 10x shift on 512 grid (right) to compare

p-t80 128 & 512

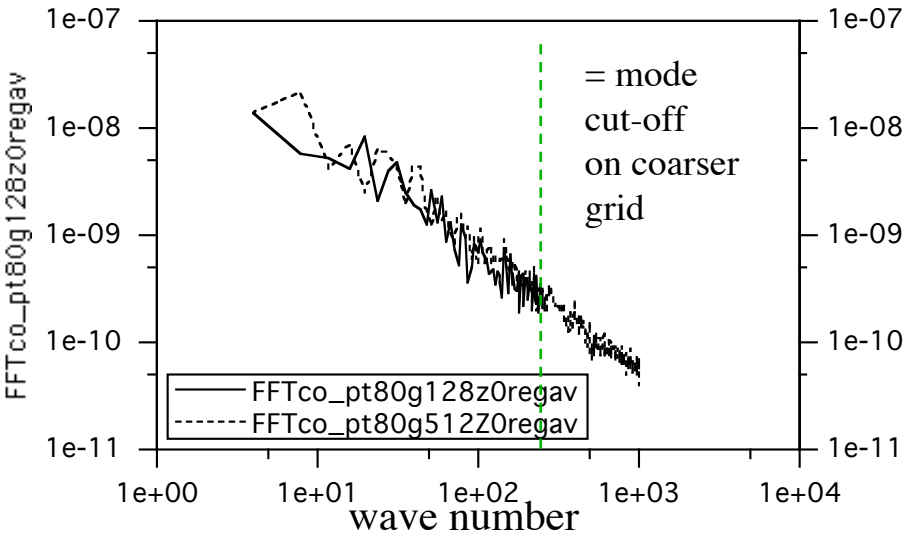

p-t80 128 & 10x p-t80 512

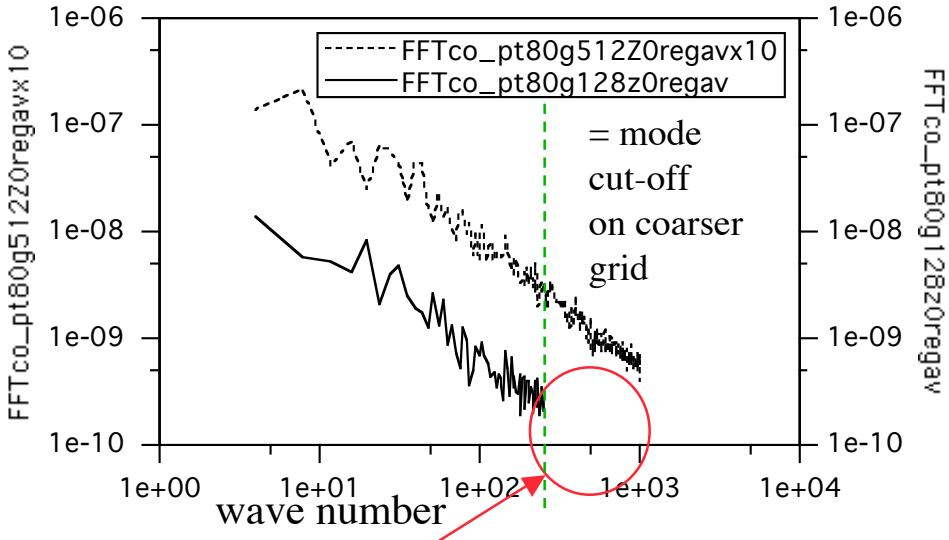

Therefore, unresolved components on 128 grid appear to be irrelevant to small k, long wavelength mode growth**.

applied physics division

Los Alamos NATIONAL LABORATORY

E.L.Vold

density, p, p1, div(u) and vorticity at late time, t= 80

velocity $\frac{\partial u}{\partial t} + u \cdot \nabla u + \frac{\nabla p}{\rho} = g$

mass continuity $\frac{\partial \rho}{\partial t} + u \cdot \nabla \rho = \rho \nabla \cdot u = \rho \dot{m}_c$

internal energy $\frac{\partial \varepsilon}{\partial t} + u \cdot \nabla \varepsilon = \frac{p}{\rho} \nabla \cdot u + (\gamma - 1) \frac{\rho_o}{\rho_o} \dot{m}_c$

density

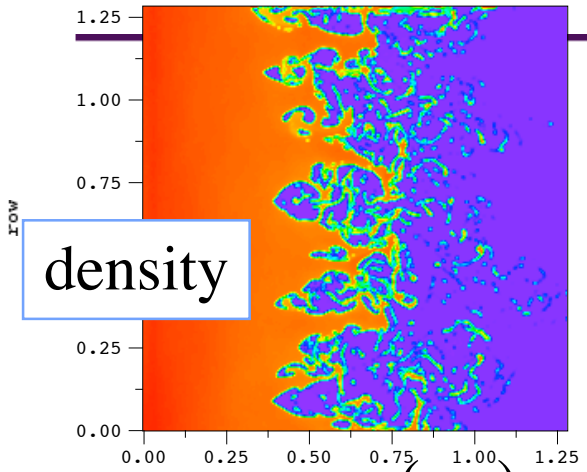

pres.=p(x,z)

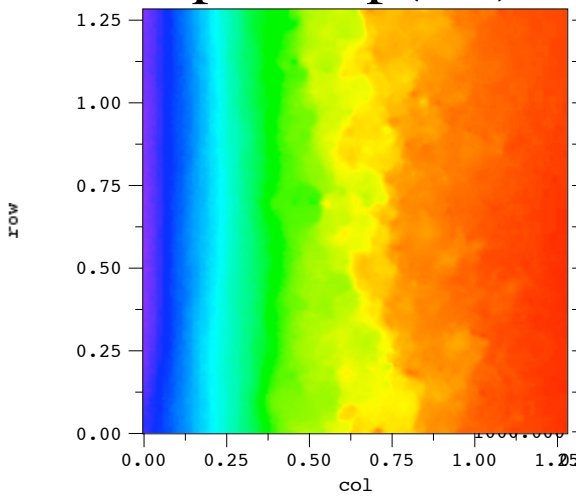

p1 = p(x,z) - p(z)

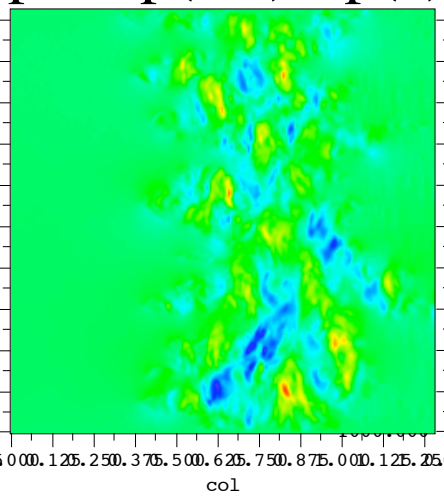

div(u)

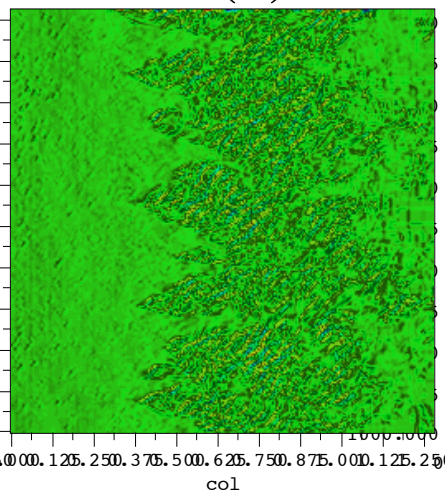

vorticity (y)

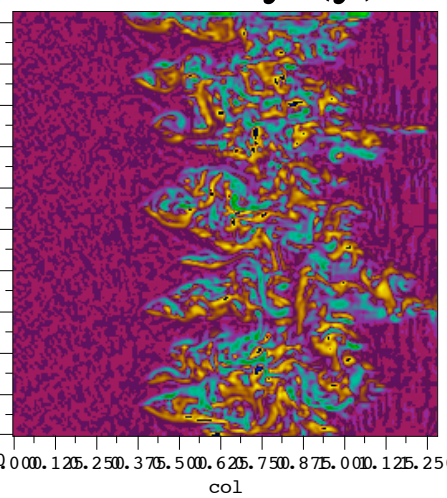

applied physics division

Los Alamos NATIONAL LABORATORY

E.L.Vold

Momentum Eqn(x) acceleration components

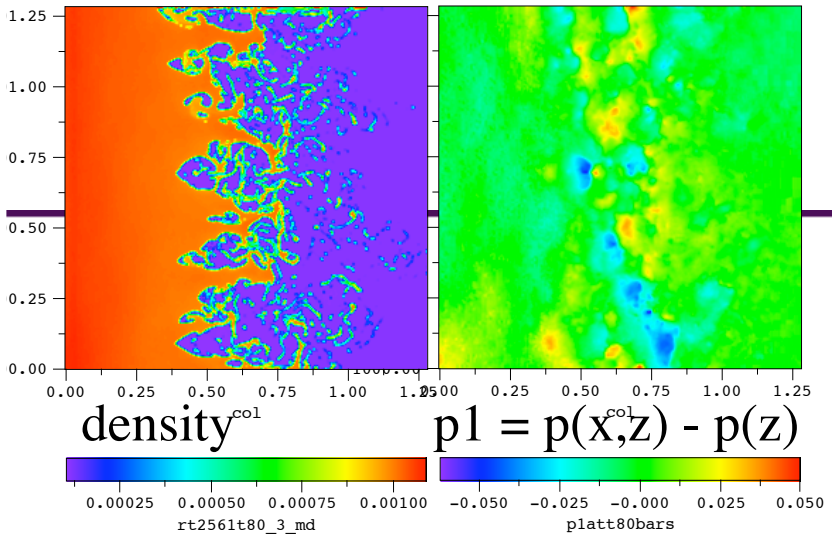

Acceleration from ρg is partitioned between all the momentum equation acceleration terms. using: $u \cdot \nabla u = \nabla u_s^2 / 2 - u \times \omega$

Mom(x): $$\frac{\partial u}{\partial t} + \frac{1}{2}\frac{\partial u^2}{\partial x} + \frac{1}{2}\frac{\partial v^2}{\partial x} - v\omega_z + \frac{1}{\rho_o}\frac{\partial p}{\partial x} = \rho g$$

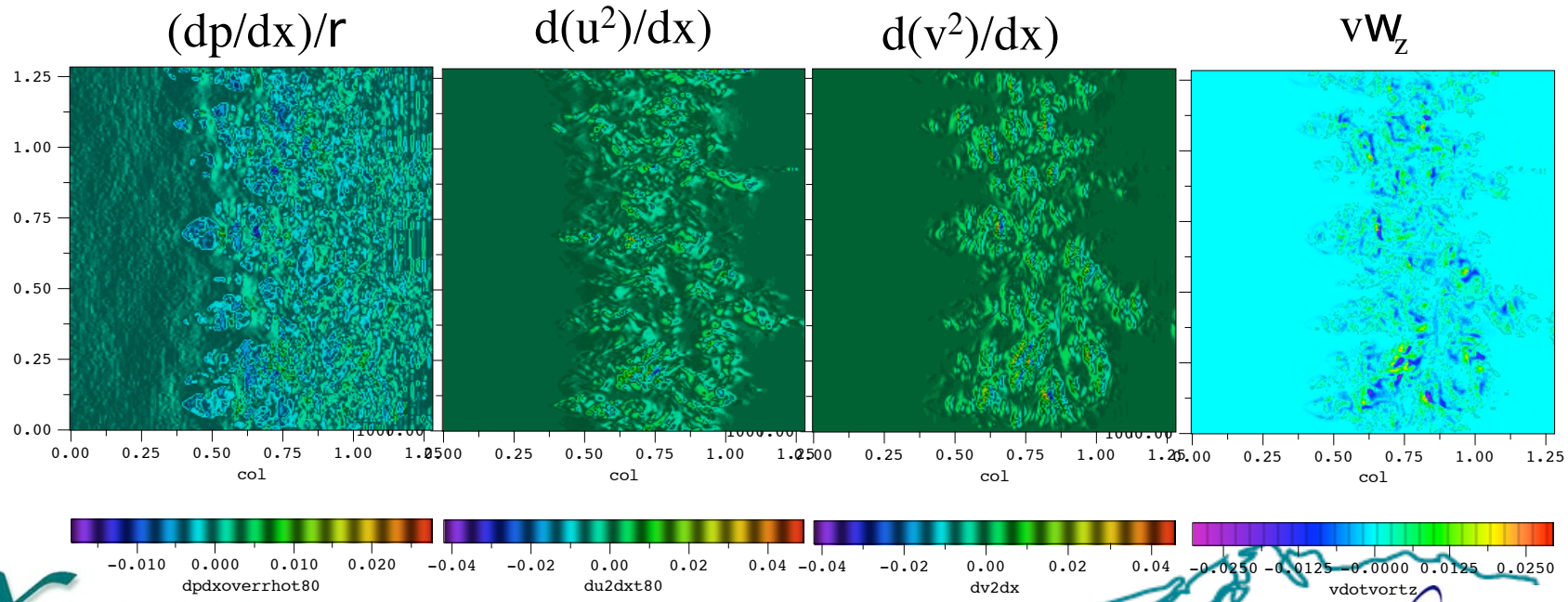

applied physics division

Los Alamos NATIONAL LABORATORY

E.L. Vold

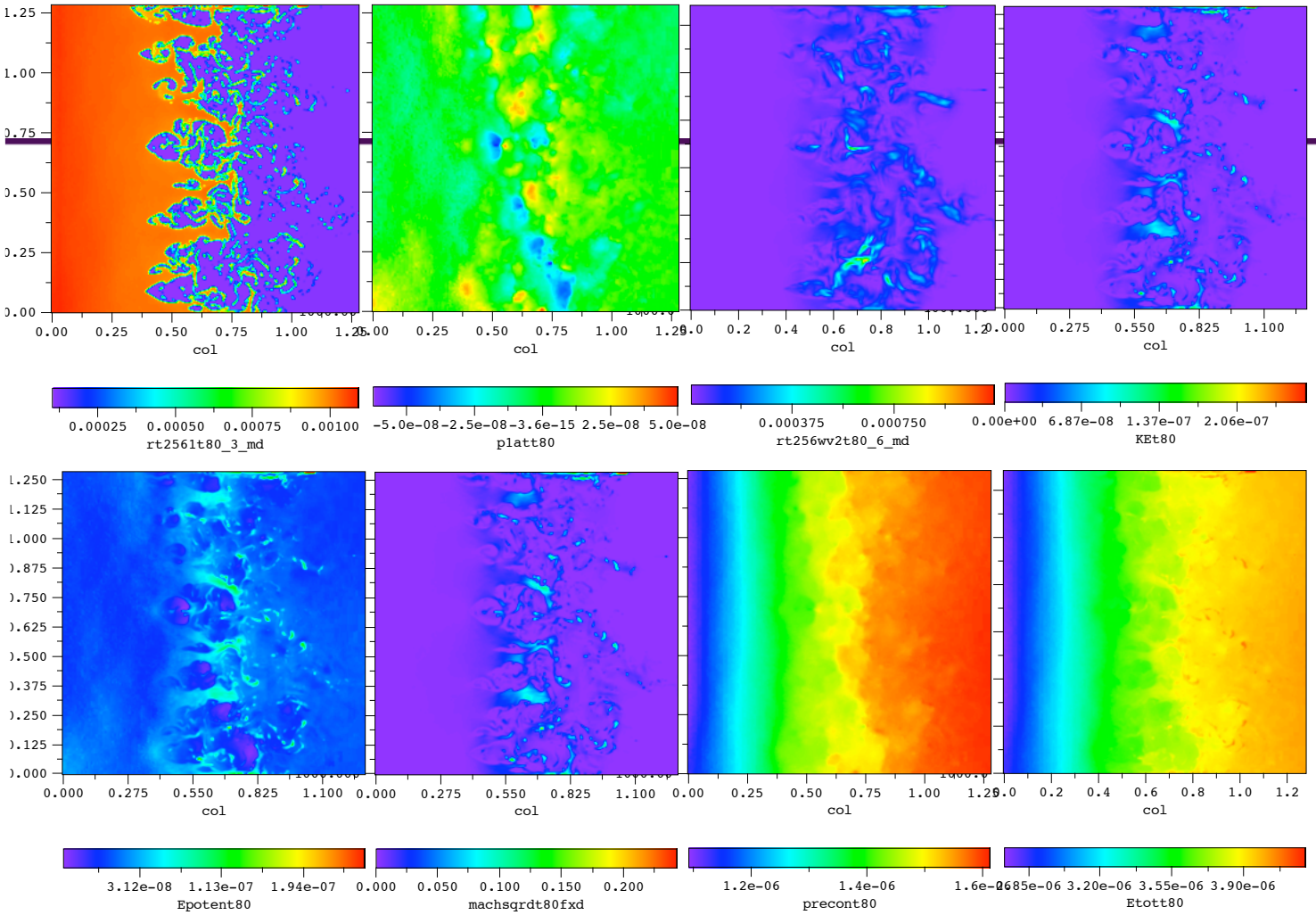

Mix layer parameters at late time showing: (across top row) density, *p1*, V^2, $KE = 0.5\rho V^2$, (across second row) *KE+p1*, Ma^2, $(\gamma-1)*\rho*e$, $Etot = \rho*(0.5V^2 + e)$. Parameters are at time, t = 80, or Z ~ 4.

E.L. Vold

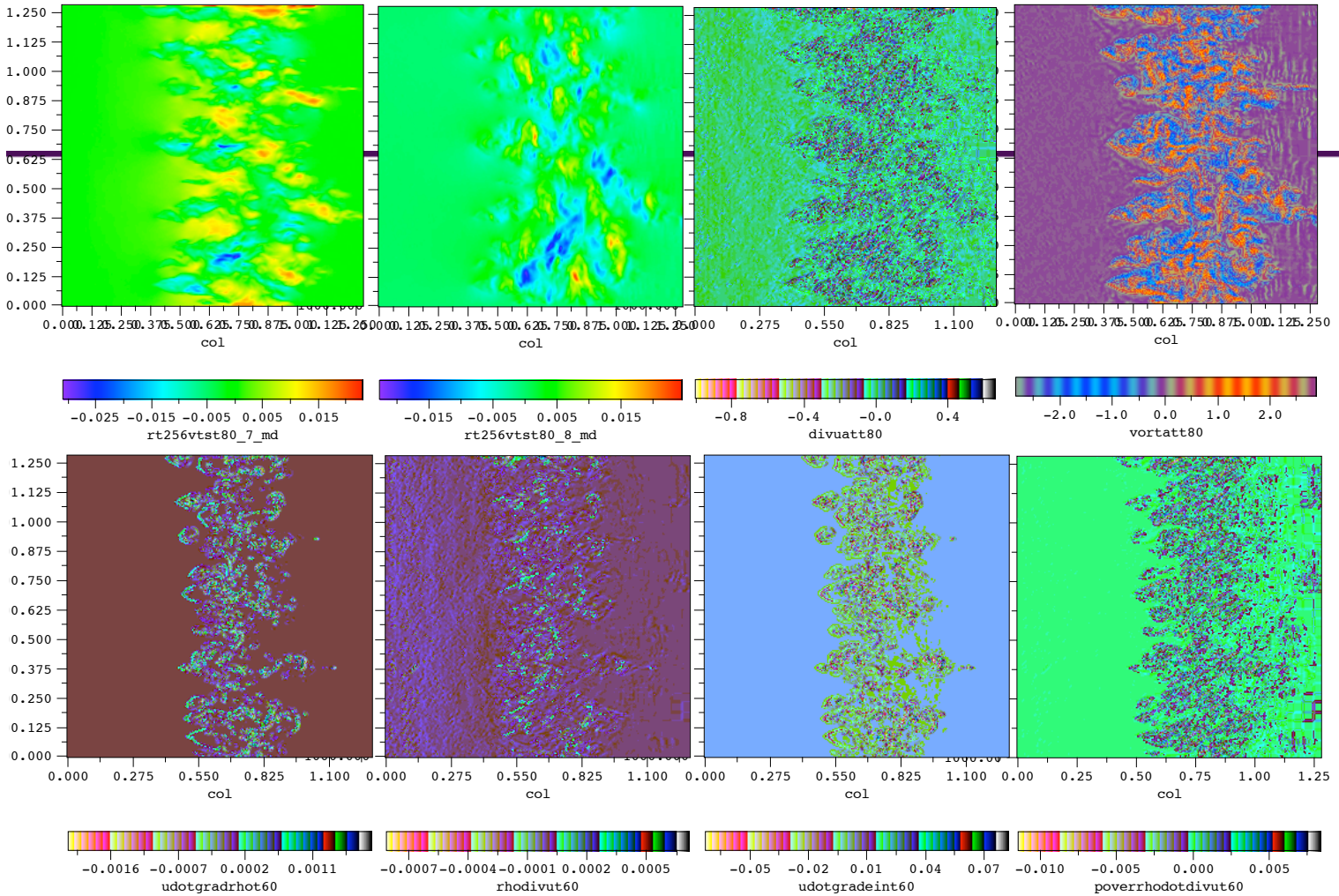

Mix layer parameters at late time showing: (across top row) u =x-component of velocity), v = y-component of velocity, *div(u)*, vorticity (z-component), and (second row) terms from the density and energy transport equations, *(u*grad)*, **div(u)*, *(u*grad)e*, and *(p/)*div(u)*. Parameters in the top row are at time, t = 80, or Z ~ 4, and the terms in the second row are evaluated at t = 60, Z ~ 2.3.

E.L. Vold

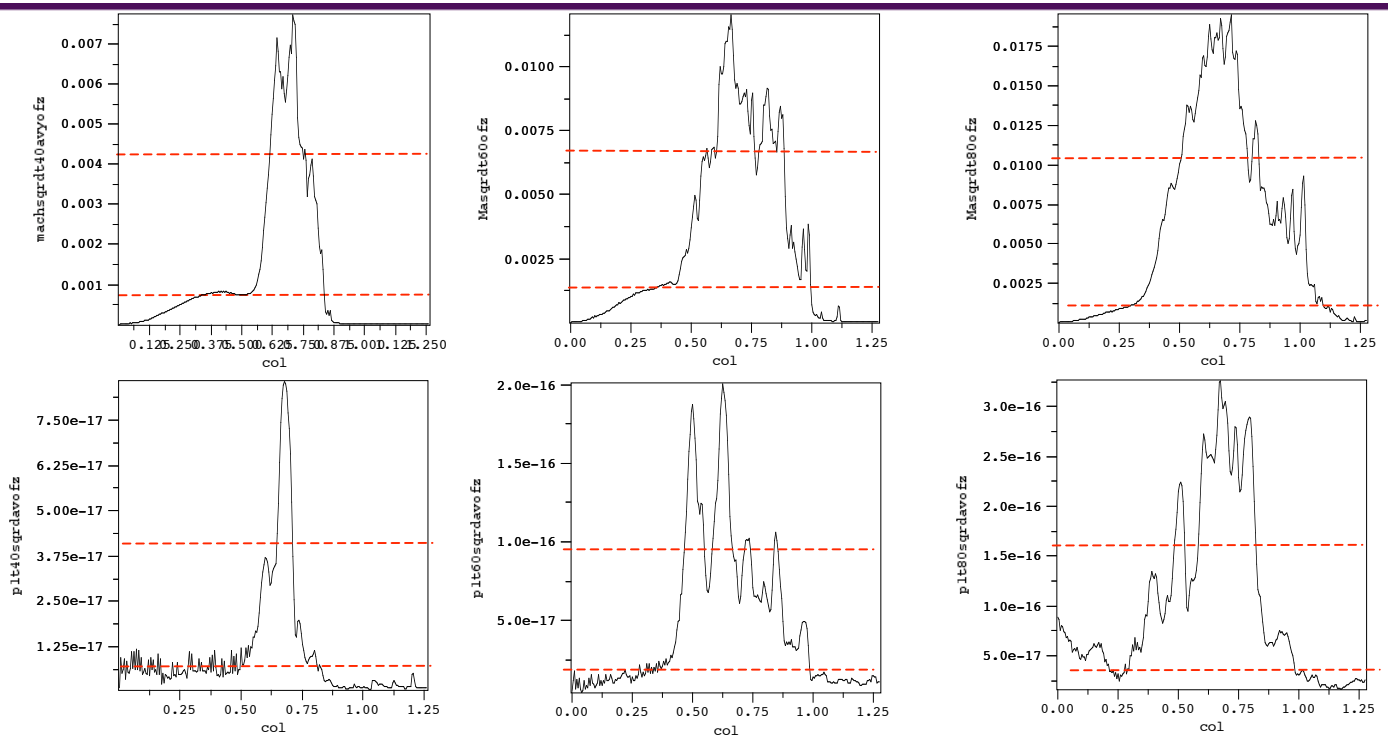

Local Mach number squared (top row) at times, t = 40, 60, 80, (Z ~ 1, 2, 4) compared to pressure fluctuations squared, $p1^2$, where $p1[x,y] = p[x,y] - p_o[x]$, and $p_o[x] = \langle p(x,y) \rangle_y$ is the transverse (y) averaged pressure, (second row) at the same three times. All values are plotted as profile averages (over y, transverse to acceleration).

E.L. Vold

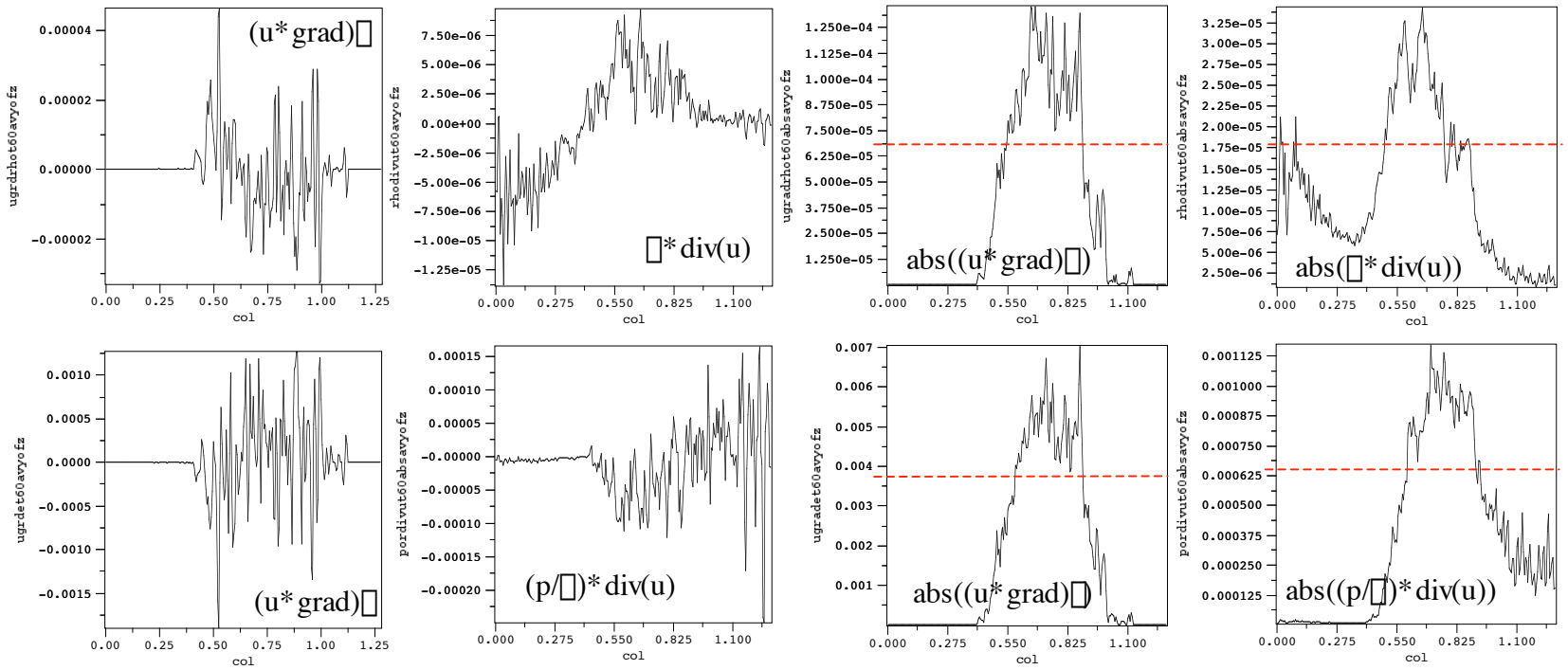

Convection and compressibility terms plotted as profile averages (averaged over y, transverse to acceleration) at late time, $t = 60$. The top row plots are for the density equation terms and the second row shows the corresponding terms for the energy equation. The four panels across either row show the profile average for the convection, *(u*grad)ρ* or *(u*grad)p*, the profile average of the compressibility term, *ρ*div(u)* or *(p/ρ)*div(u)*, and then the magnitude (absolute value) of these terms, *abs((u*grad)ρ)* or *abs((u*grad)p)*, in the third panels, and, *abs(ρ*div(u))*, or *abs((p/ρ)*div(u))* in the fourth panels. The mix layer width at this time is identifiable in the convection plots (panels 1 or 3) where the convection terms go to zero. The horizontal dashed lines (panels 3 and 4) estimate the profile average value within the mix width.

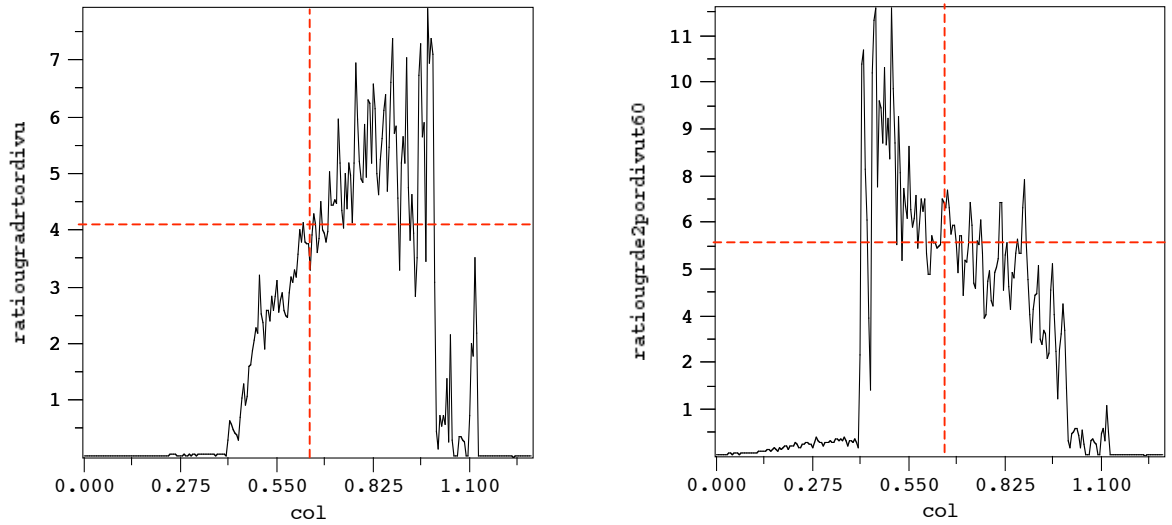

Ratios, R, for density (left) and internal energy (right) of profile averaged magnitude of the local convection relative to the compressibility terms at late time, t = 60 (corresponding to results in previous figure). The left plot (density equation terms) shows the ratio, R_r = $\langle abs((u*grad)\rho)\rangle / \langle abs(\rho*div(u))\rangle$ (averaging over y, transverse to acceleration). The right plot shows the corresponding ratio for the internal energy equation terms, R_e = $\langle abs((u*grad)\rho)\rangle / \langle abs((p/\rho)*div(u))\rangle$.
The vertical dashed lines signify the location of the interface initially (t =0), and the horizontal dashed lines estimate the profile average value within the mixed region width.

E.L.Vold

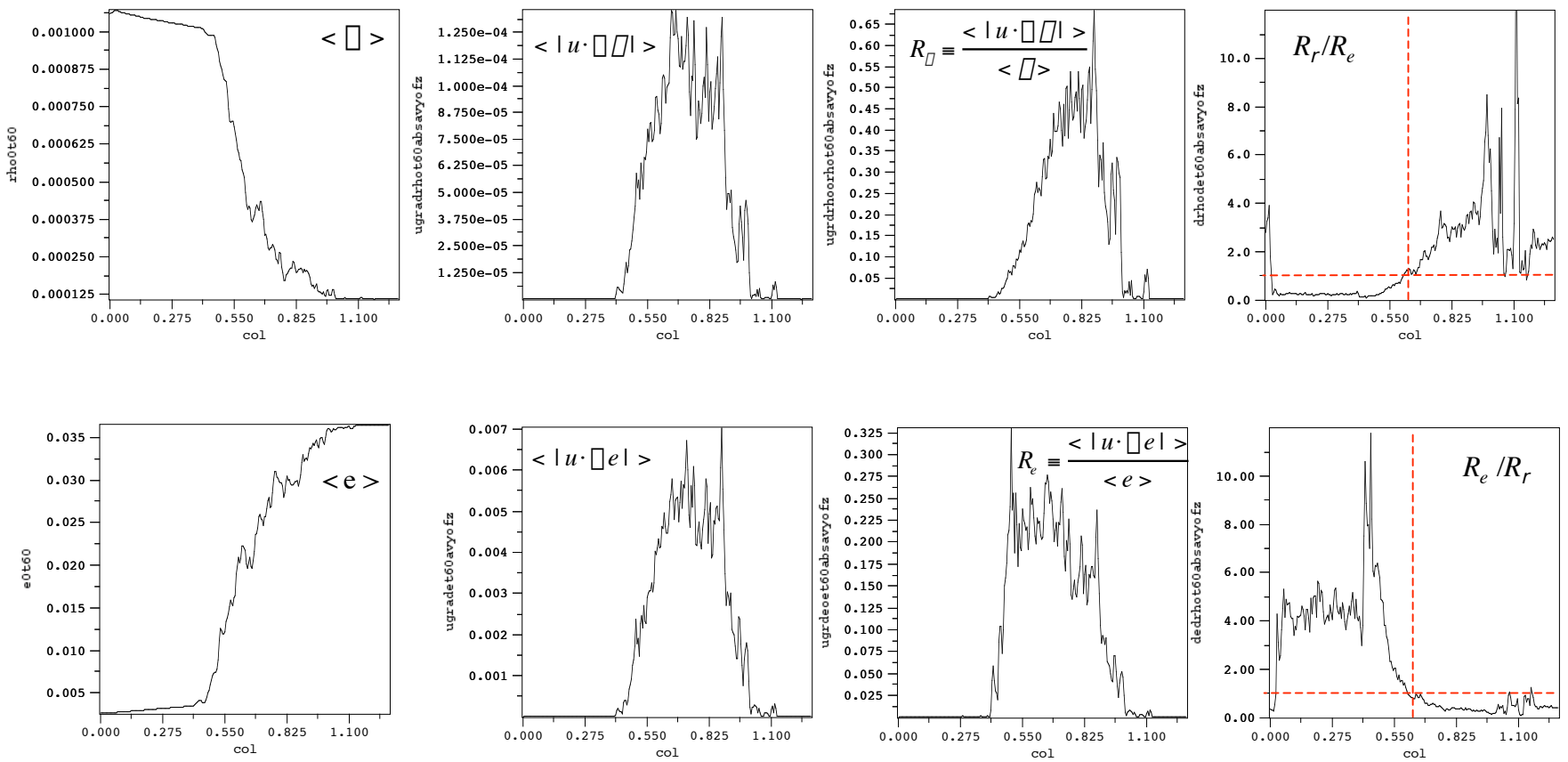

Plots to evaluate the relative magnitude of the contribution to pressure fluctuations due to the convection of density verses energy, showing density parameters across the top row, and internal energy in the bottom row. Across each row the panels show profile average, profile average magnitude of convection, e.g., *(abs((u*grad)ρ))* for density, and a ' convective rate of change', equal to the ratio of plot 2 to 1 (e.g., for density, $R_r \sim (d\rho dt/\rho)$ without compressibility effects for density in top row). Panel 4 (top row) is the ratio of plot 3 for density to plot 3 for internal energy, thus compares this convection rate for density to the convection rate for internal energy. Panel 4 bottom row is the inverse ratio to show where the internal energy convection rate is more important. In panel 4 plots, the vertical dashed line signifies the location of the interface initially (t=0), and the horizontal dashed line at one shows where the magnitudes of density and energy fluctuations are comparable.

E.L. Vold

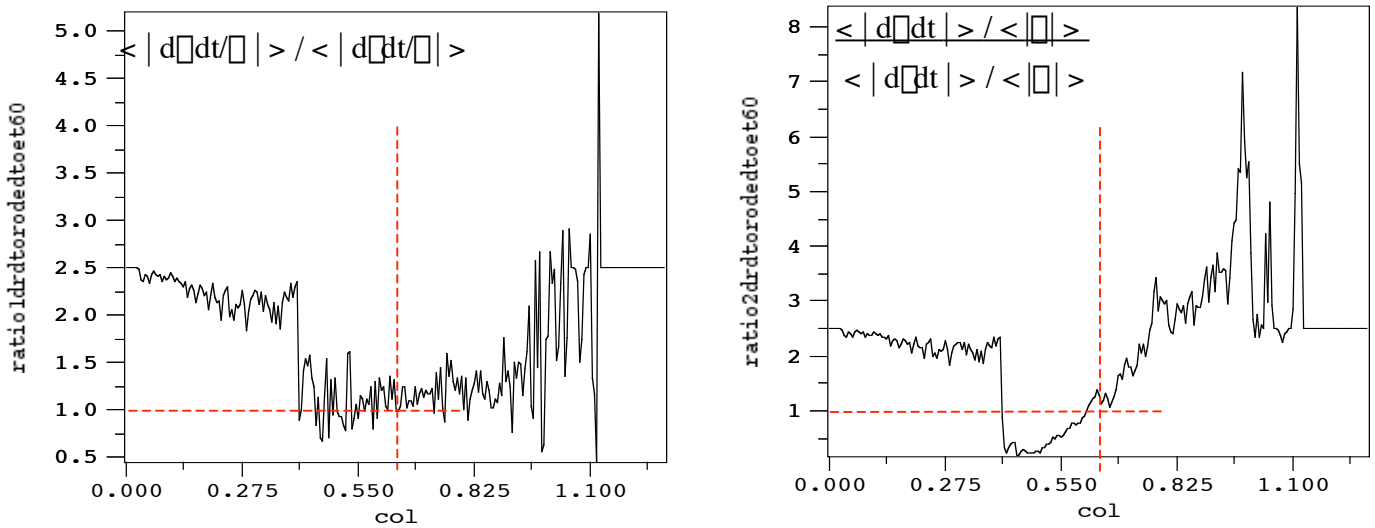

Two profile averages for the relative magnitude of the density and internal energy fluctuations along x (col). These drive the pressure fluctuations and thus the mix layer growth. The vertical dashed line signifies the location of the interface initially (t=0), and the horizontal dashed line at one shows where the magnitudes of density and energy fluctuations are comparable.

Pressure fluctuations, p_1, coupled to hydrostatic grad p

Pressure gradient fluctuation by components, dp/dz, dp_1/dz and dp_1/dy (z-axial, and y-transverse) suggest fluctuations are coupled to the hydrostatic pressure gradient (steepest in the unmixed heavy fluid to the left of the mix region) and cascade down through the mix layer into fluctuations and then into the transverse components.

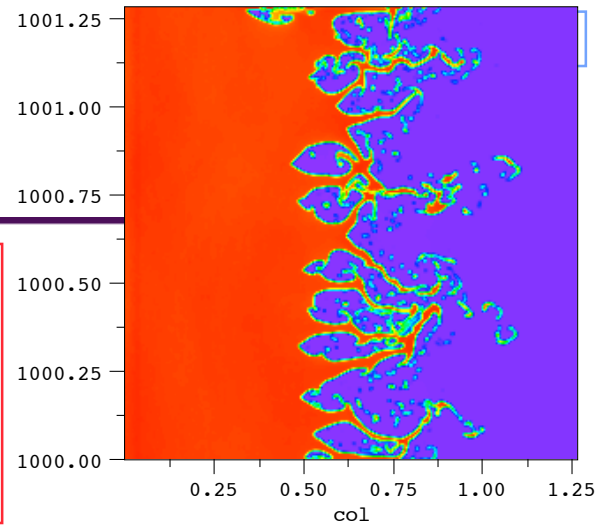

$\langle |dp/dz| \rangle_y$

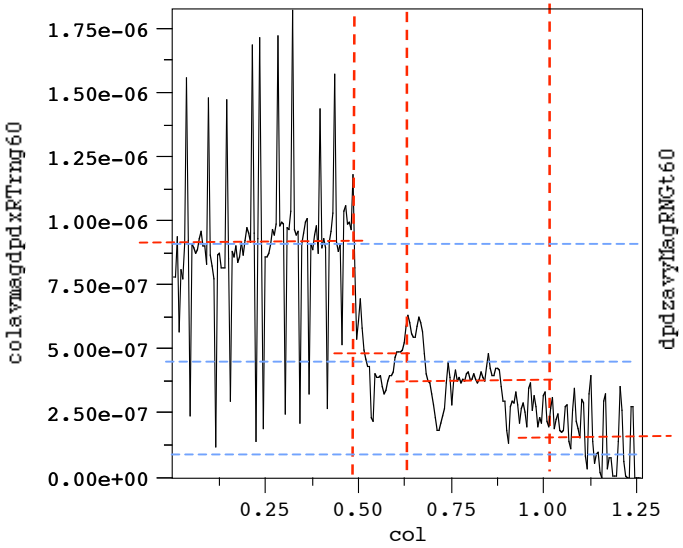

$\langle |dp_1/dz| \rangle_y$

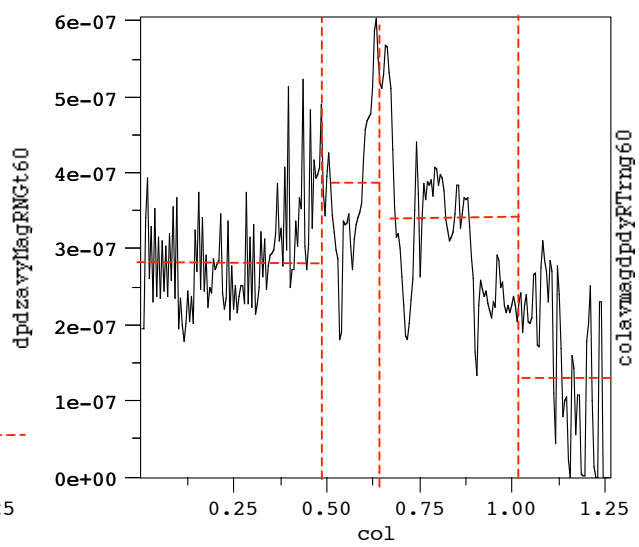

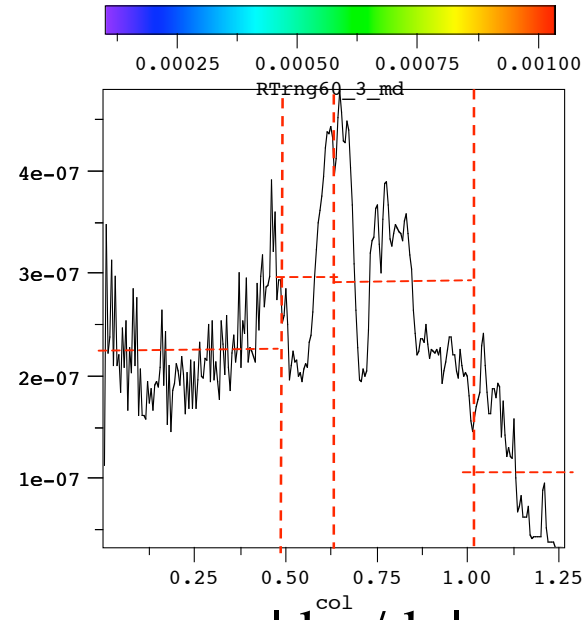

$\langle |dp_1/dy| \rangle_y$

Dpdz Averages from .xcl = 9.1, 4.4, 3.5, 1.47

Dpdy Averages from this plot = 2.26, 2.89, 2.81, 1.02

Dpdz Averages from .xcl(edge2) = 9.0, 5.1, 3.6, 1.5

Dpdz Averages from .xcl (edge2 w/ -5pt boumdary) = 9.0, 4.2, 3.5, 1.5

applied physics division

case: rngt60

Los Alamos NATIONAL LABORATORY

E.L.Vold

Late time density and pressure fluctuation, p'- compressible vs. incompressible* computations

Compressible calculation

Density

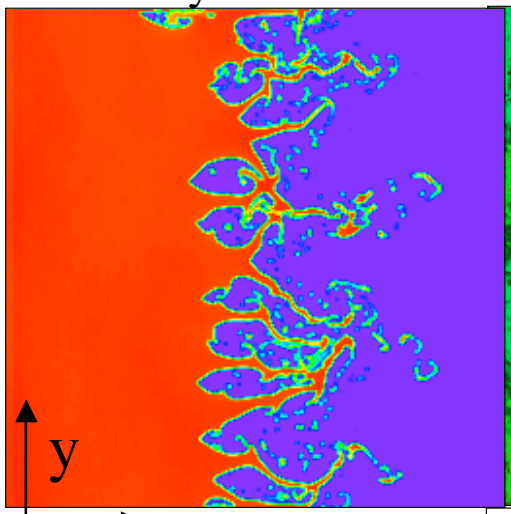

Pressure fluctuation

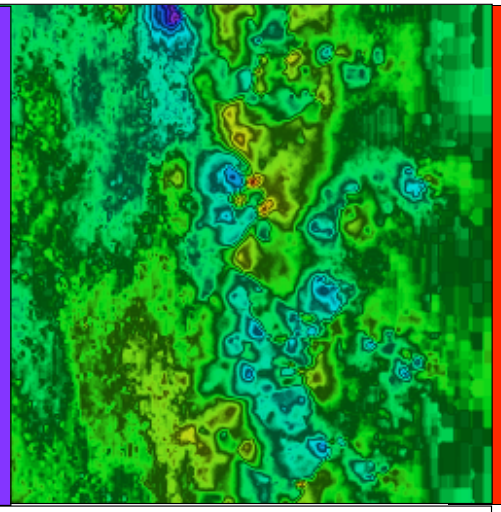

g = - g**x**

Incompressible calculation

Density

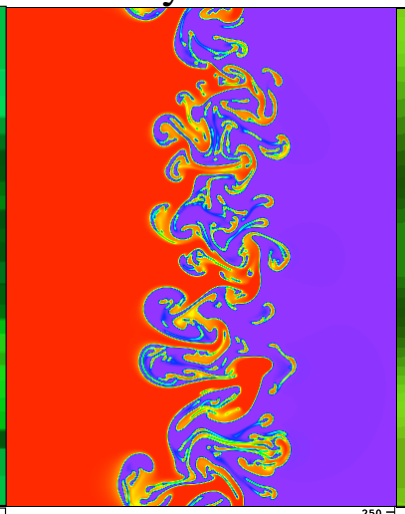

Pressure fluctuation

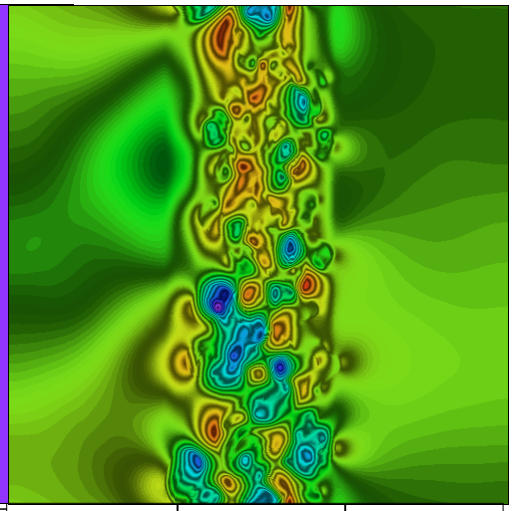

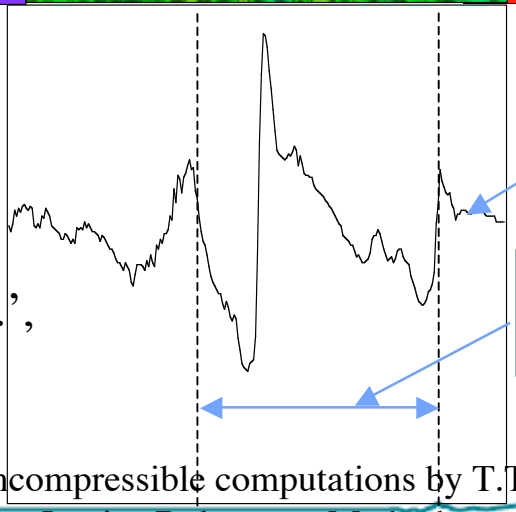

‘typical’ profiles p'(x)

Mix width from Density profiles

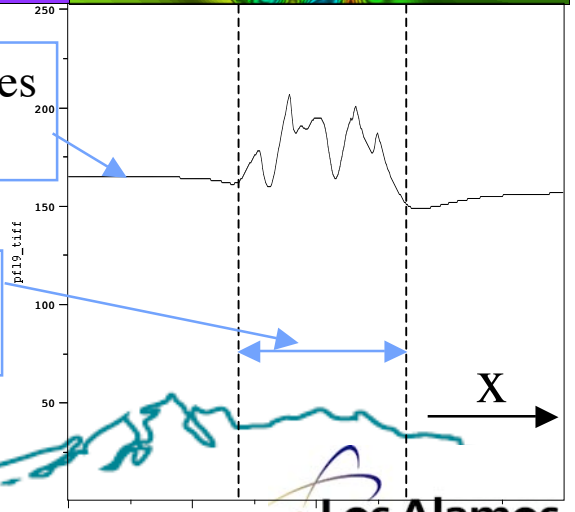

Pressure fluctuation
$p'(x,y) = p(x,y) - p_h(x)$
with ‘hydrostatic equilib.’,
$p_h(x) = \langle p(x,y) \rangle_y$

applied physics division

* incompressible computations by T.T.Clark using Lattice Boltzmann Method

Los Alamos NATIONAL LABORATORY

Compressible vs. Incompressible Dpdz

Dpdz-ave.transverse Magnitude $\langle|dpdz|\rangle_y$

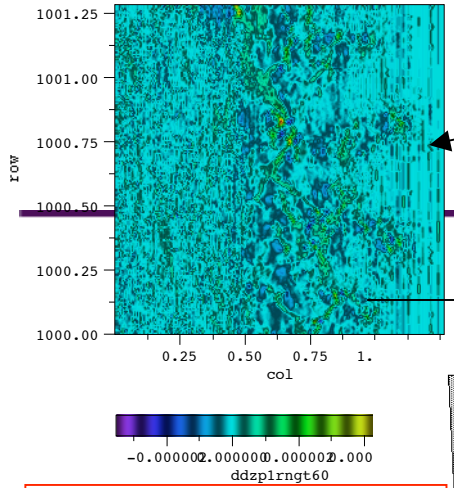

z

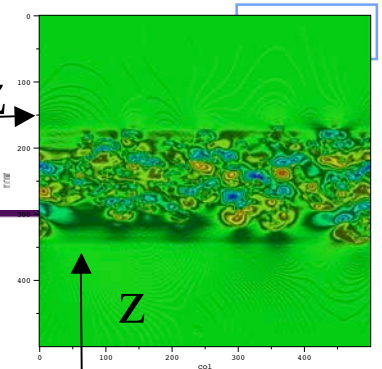

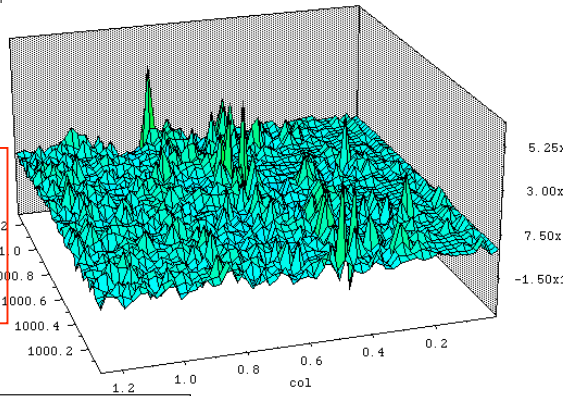

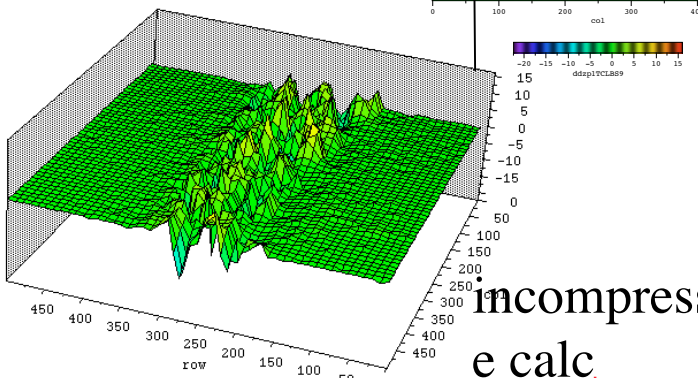

Mix layer growth is by fluctuations, here seen in dp'/dx.

compressible calc

incompressible calc

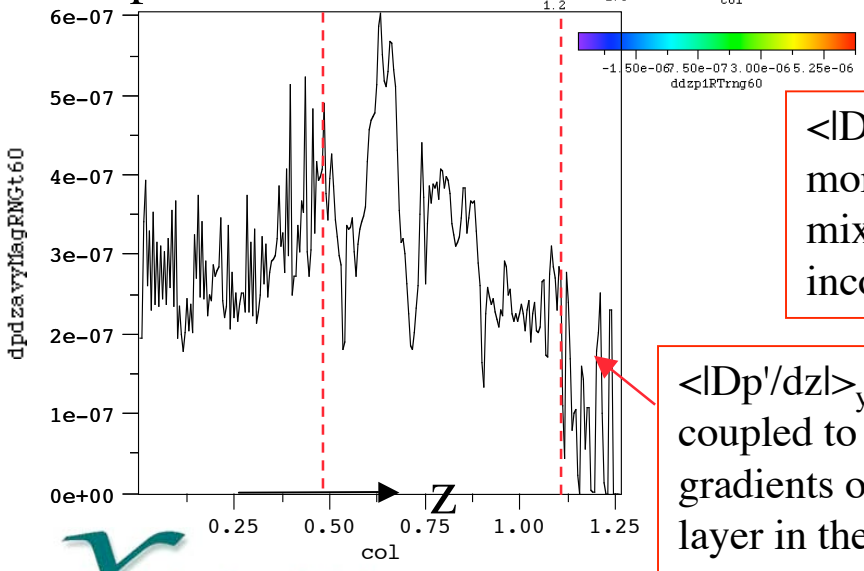

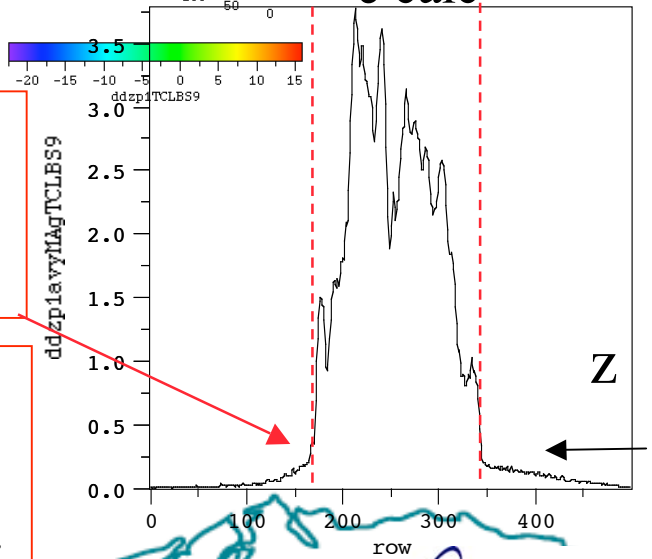

$\langle|Dp'/dz|\rangle_y$ is much more localized within mix layer in the incompressible calc.

$\langle|Dp'/dz|\rangle_y$ appears to be coupled to the hydrostatic gradients outside the mix layer in the compressible calc.

applied physics division

Los Alamos NATIONAL LABORATORY

Pressure fluctuation field Compressible (left) vs incompressible (rt)

E.L.Vold

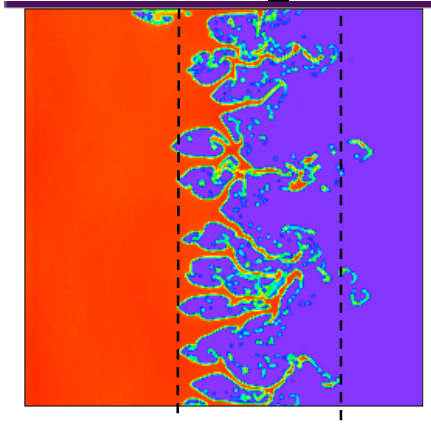

Thermodynamic pressure: source in fluctuating densities and internal energy.

Kinetic pressure potential: source in mix region where u.ne.0.

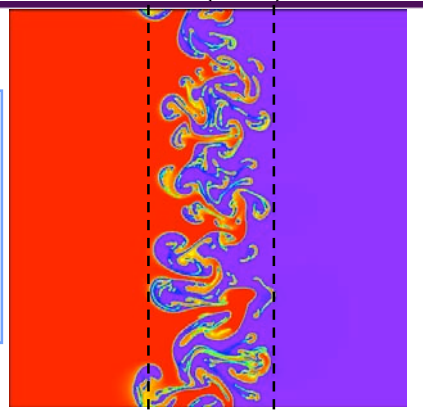

$$\nabla p = (\gamma - 1)\rho\nabla\varepsilon + (\gamma - 1)\varepsilon\nabla\rho$$

$$\nabla \cdot (\rho^{-1}\nabla p) = \nabla \cdot (u \cdot \nabla u + \nu\nabla^2 u)$$

$p_{src}[\nabla \cdot u => 0]$

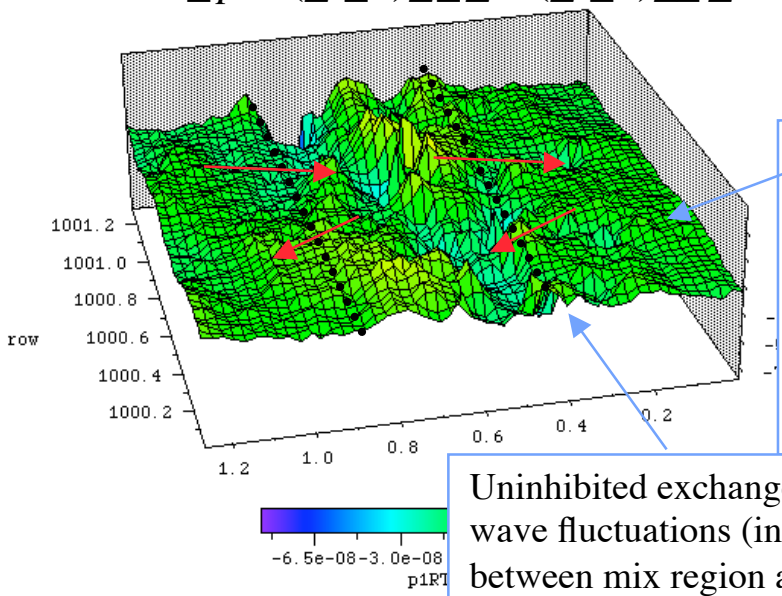

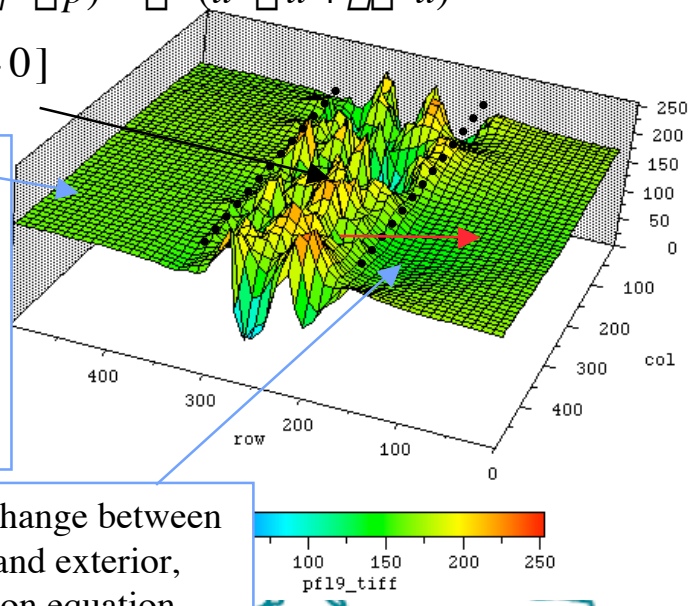

'Exterior region' (unmixed) where long wavelength small amplitude perturbations coincide with BC imposed at 'box scale lengths'.

Uninhibited exchange via wave fluctuations (in ρ or e) between mix region and exterior region long wavelength perturbations.

Limited exchange between mix region and exterior, due to Poisson equation for kinetic potential pressure, p

applied physics division

Los Alamos NATIONAL LABORATORY

E.L.Vold

Summary: compressibility issues in R-T mix

- Observations in comparing experimental and computed R-T mix rates
  - R-T multi-mode growth rate characterized with mix width, $h = \alpha A g t^2$
  - $\alpha_{computed} < \alpha_{experimental}$ => may be compressibility ($\alpha_{computed} \sim \alpha_{experimental}$ for 'front tracking' and for the present multi-fluid method - similarity in methods may be retaining two compressible fluid states at interface)
- Methods: compressible vs. incompressible
  - P[ρ,ρ] - compressible computation -pressure is true thermodynamic quantity coupled to two 'wave equations, one for density and one for energy
  - P[div*u] - incompressible computation - pressure is dynamic variable = f(u), weak dependence upon ρ
  - Multi-fluid methods retain complete fluid states on each side of interface - some compressible methods may retain density discontinuity with an averaged energy at the interface. Without energy discontinuity, pressure fluctuations may be reduced as: $p \sim \rho_o \rho + \rho_o \rho$
- Results: Fluctuation Quantities
  - Gallery of fluctuation quantities, p, u, v, E, ρ, $\rho \cdot u$, etc….
  - FFT components, Mix layer profile averages, Dp/dz distributions in compressible and incompressible

Summary: Consistent picture of compressibility in R-T mix

E.L. Vold

- Consistent picture of role of compressibility in R-T multi-mode mix layer growth rates:
  - pressure fluctuations are enhanced within mix layer due to compressibility and energy fluctuation contributions
  - pressure fluctuations are less restricted to mix layer in compressible waves between mixed and unmixed regions
  - evidence that pressure fluctuations are coupled to hydrostatic pressure gradient only in the case of compressible fluid.
  - hypothesized that in the compressible case more fluctuation energy is exchanged between the mix layer and the unmixed region where long wavelength perturbations reside for consistency with the boundary conditions.
  - hypothesized that energy in these long wavelength perturbations in unmixed region are transported into mix region more efficiently in the compressible fluid.
  - more energy in longer wavelength perturbations within the compressible mix layer yields a faster growth rate consistent with experimental values.